203

57P.
$3.00

DOWNEY PLANT

RESEARCH AND ENGINEERING DIVISION

THE ATOMIZATION OF A SOLUTION OF 2, 4-DIHYDROXYBENZOPHENONE IN BIS (2-ETHYLHEXYL) HYDROGEN PHOSPHITE

A Special Report

Under

Contract DA-18-108-405-CML-829

Report 0395-04(20)SP / May 1964 / Copy 24

AEROJET GENERAL TIRE GENERAL

AEROJET-GENERAL CORPORATION

DOWNEY, CALIFORNIA

AEROJET-GENERAL CORPORATION
Research and Engineering Division
11711 Woodruff Avenue
Downey, California

THE ATOMIZATION OF A SOLUTION OF 2, 4-DIHYDROXYBENZOPHENONE IN BIS (2-ETHYLHEXYL) HYDROGEN PHOSPHITE

by

R. E. Brown

Investigations Under U. S. Army Chemical Center

Contract DA-18-108-405-CML-829

0395-04(20)SP

Reviewed by R B Mortensen
R. B. Mortensen, Head
Terminal Ballistics Dept
Research Division

Date: 6 May 1964

No of Pages: 53

Approved by A. E. Dahlstrom for
H. J. Fisher, Head
Research Division

Classification: UNCLASSIFIED

ACKNOWLEDGMENT

The author acknowledges the contributions that A Armstrong and K Harris made in preparing this report particularly in the experimental phases

SUMMARY

An experimental study was made of the drop-size distributions obtained on injecting a liquid solution composed of, by weight, 15% 2, 4-dihydroxybenzophenone in 85% bis (2-ethylhexyl) hydrogen phosphite into nitrogen gas streams at sonic velocity The liquid solution was introduced into the gas stream through a single injector and through triple injectors Variations were imposed in the flow rates of both liquid and gas, and in the temperature of the gas The collected aerosol droplets were sized, counted, and described mathematically using a modified form of the logarithm (log)-probability distribution function (Reference 1) The parameters of the distribution function are shown to vary directly with the flow rate ratio of liquid to gas

Equations were determined showing the variance of the two log-probability parameters These equations were developed using the same form as that of the Nukiyama-Tanasawa relationship (Reference 2). This extension of the Nukiyama-Tanasawa equation enables predicting the particle-size distribution rather than just a mean diameter of the distribution

The experimental data are also shown to generally agree with the results of other investigators

CONTENTS

ILLUSTRATIONS

ILLUSTRATIONS (Continued)

TABLES

1. INTRODUCTION

In this investigation, it is attempted to describe some of the important parameters of a pneumatic atomization process in which a gas at elevated temperatures is used as one of the components of the system; and the second component is a solution. The effect of the important parameters on a distribution function are emphasized.

A liquid jet exiting from a restricted orifice will have oscillatory disturbances caused by surface instabilities. These initial disturbances may result from one or more of the following factors:

a Surface tension

b. Inertia forces

c. Imperfections of the nozzle orifice

d Turbulence of the liquid

e. Effervescence of a dissolved gas or liquid or solid impurities

All of these factors may occur simultaneously or overlap one another. These disturbances, without the aid of any other force, result in droplet formation because of the restoring properties of surface energy. The droplets formed, or which could be postulated from disturbances in the liquid jet, can then be considered to be the maximum sizes introduced into the gas stream.

The gas stream can then fracture existing droplets, or the liquid jet, both of which are products of the initial jet instabilities. In so doing, smaller droplets are formed, and if the gas has a higher temperature than the liquid, initially some vaporization of the liquid will result. In a system in which solutions are involved and assuming that eutectic mixtures are not present, the component having the lowest specific heat will be vaporized first. This leads to droplets of different compositions and solid particles that were initially dissolved or suspended.

It is therefore apparent that in most atomization processes a range of particle sizes is produced. In describing the droplet sizes it is desirable to have a method that not only completely describes the distributions but also relates changes in distributions to the physical properties influencing the breakup mechanism.

An experimental study was made of the drop-size distributions resulting from spraying a solution composed of 15% 2, 4-dihydroxybenzophenone in bis(2-ethylhexyl) hydrogen phosphite. The flow-rate ratios of gas-to-liquid (solution) were varied as well as the initial temperature of the gas (nitrogen) and the method of liquid injection into the gas stream.

2. EXPERIMENTAL TECHNIQUES

2.1 HOT-GAS FURNACE

An electrically heated hot-gas furnace (Figure 1) was employed to supply nitrogen gas for atomization. This gas source was used in cold and hot gas experiments. This furnace consists of a center pebble bed column. The pebble bed and the column are composed of 99.9% aluminum oxide. Surrounding the ceramic column are four U-shape molybdenum disilicide (Kanthal-Super) heating elements. These elements transfer energy to the pebble bed. This energy is, in turn, transferred to the passing gases.

The furnace has three different zones of composition firebrick and is also insulated so that at maximum operating temperatures (between 2500 and 3000°F) the temperature of the furnace wall never exceeds 200°F. Thermocouples and pressure transducers are located at various places so that the temperature and pressure can be both monitored and automatically controlled.

2.2 ATOMIZATION

The liquid being atomized is stored in a constant displacement injector (Franklin Institute, Reference 1). The injection into the gas stream takes place outside the furnace (Figure 2). The gas from the furnace emits from a venturi nozzle and mixes with the liquid being injected perpendicularly to the gas stream, through a 0.027-in. tube. Three liquid injectors were also employed to determine if any difference in particle-size distribution would result when this type of injection replaced a single injector.

2.3 AEROSOL ASSESSMENT

The liquid solution was atomized through a short duct, approximately 6 in. diameter and 3 in. long, into an aerosol test chamber (21.5 ft diameter by 24 ft high)(Figure 2). Glass slides placed on the chamber floor before the test began were used to collect the droplets that fell from the aerosol cloud. The sampling period for all of the tests was 30 min, enough time according to Stokes equation, for all particles equal to or larger than 7 μ to fall out. At the end of this period a 6-min air sample was taken and collected on millipore filters to determine the mass fraction of airborne droplets. Approximately 4 cubic feet of air were sampled.

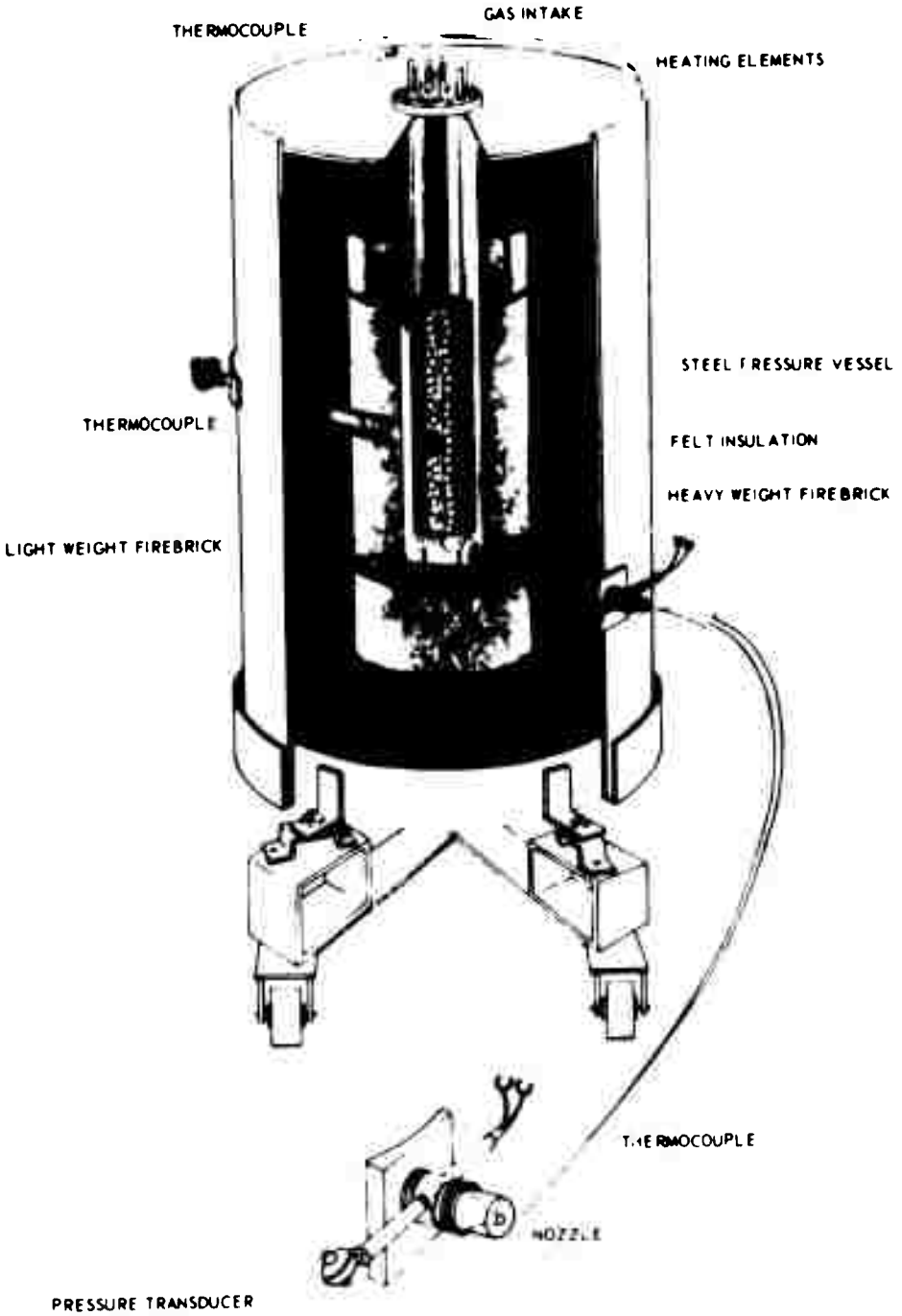

Figure 1. Electric Furnace.

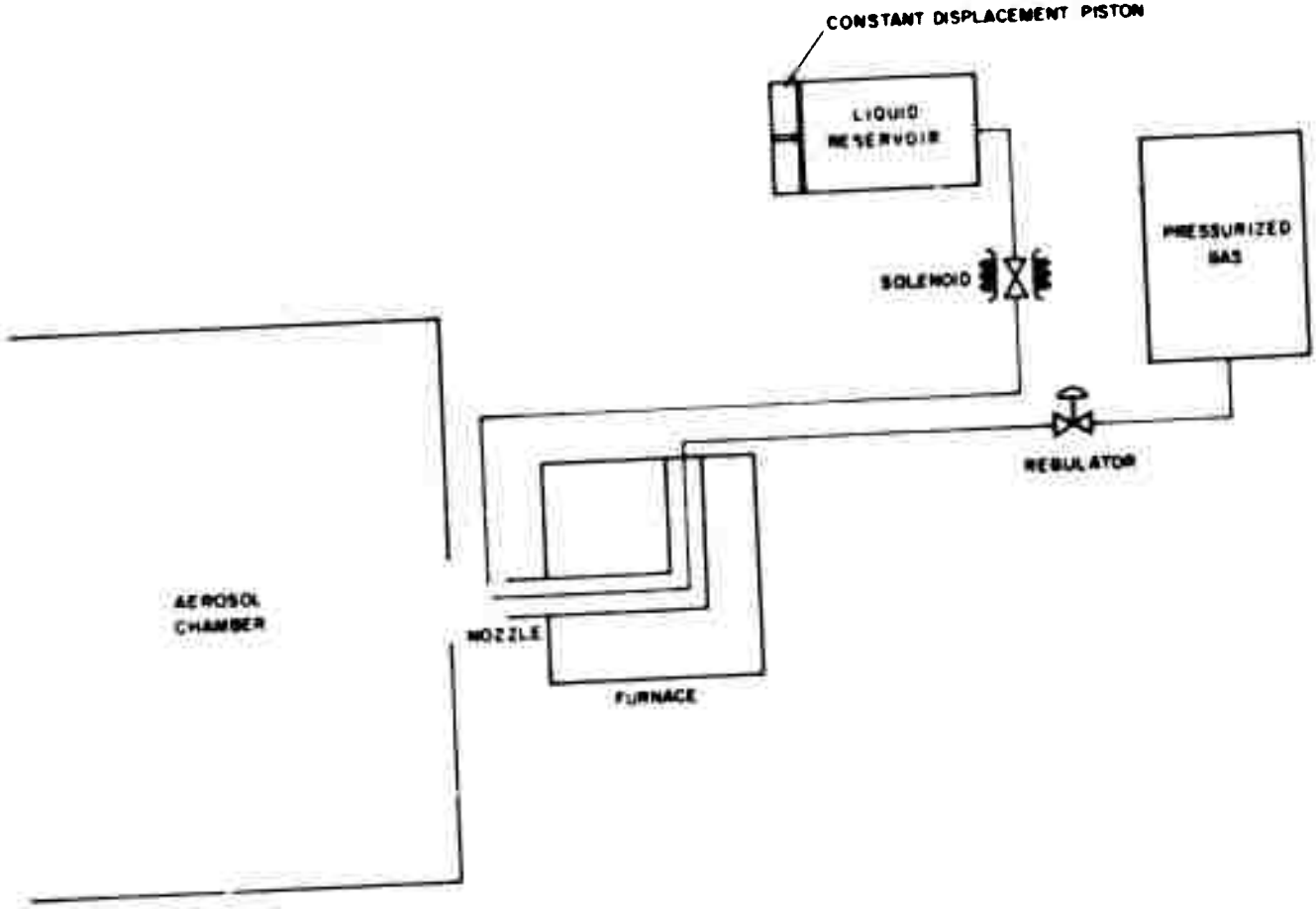

Figure 2 Assembly for Thermal Atomization

2.4 PARTICLE-SIZE DISTRIBUTIONS

The microscope slides containing the droplets were photomicrographed under a 37.5 magnification. These photomicrographs were then projected onto a screen and manually counted by using a pair of electronic calipers. Each experiment was counted by at least two counters. Each counter analyzed half of an experiment.

The spread factor of the 15% solution of 2,4-dihydroxybenzophenone in bis(2-ethylhexyl) hydrogen phosphite was determined at many different droplet sizes. The mean spread factor of the solution was 0.430 ± 0.015 for 52 individual determinations. The spread factors were determined by directly measuring the height and diameter of the lens-shaped droplets on microscope slides coated with Aerosol O-T* solution. The volume of the lens and the diameter of the sphere with the same volume were then computed. The ratio of the spherical diameter-to-lens diameter is the spread factor.

The particle-size distributions were then fitted to mathematical functions (Reference 2). Both the Weibull,

$$Y = 1 - \int_0^x e^{-\left(\frac{x-\gamma}{\alpha}\right)^{\beta}} dx \qquad (1)$$

and the logarithm-probability functions were considered

$$Y = \frac{1}{2\pi \ln\sigma} \int_0^x e^{-\frac{(\ln x - \ln \bar{x}_n)}{2 \ln^2 \sigma}} d\ln x \qquad (2)$$

where Y is the cumulative fraction of droplets having a diameter equal to or less than x. α, β, and γ are distribution parameters as are $\bar{x}$ and σ however the latter two are the geometric mean and standard deviation of the geometric mean, respectively.

2.5 CHEMICAL ANALYSIS

Both the glass slides and millipore filters were assayed for bis** and uvinul*** The procedures used are discussed in References 3 and 4

*Fisher Chemical Co., New York, N.Y.
**Bis will refer to bis(2-ethylhexyl) hydrogen phosphite
***Uvinul will refer to 2,4-dihydroxybenzophenone Uvinul-400 is the commercial name for this compound

3 DISCUSSION OF RESULTS

It was found that all of the distributions could be described by both the Weibull and modified logarithm-probability functions (Reference 2). The cumulative frequency data could be reproduced by both equations to within 0.82%.

No relationship between the parameters of the Weibull distribution and the experimental conditions of the atomization study could be found. Relationships were found, however, between both modified parameters of the log-probability function and the flow-rate ratio of liquid to gas. All of the results are therefore based on the log-probability distribution.

3.1 DISTRIBUTION PARAMETERS

The logarithm-probability function is defined by,

$$Y = \frac{1}{\sqrt{2\pi}\,\ln\sigma} \int_0^x e^{-\frac{(\ln x - \ln \bar{x})^2}{2\ln^2\sigma}} \, d\ln x \qquad (3)$$

where

$$\ln \bar{x} = \frac{\Sigma f_i \ln x_i}{\Sigma f_i}, \text{ the geometric mean} \qquad (4)$$

and

$$\ln^2\sigma = \frac{\Sigma f_i (\ln x_i - \ln \bar{x})^2}{\Sigma f_i}, \text{ the variance about } \ln \bar{x} \qquad (5)$$

Y is the cumulative fraction of particles.

When Equations 4 and 5 were used to define the cumulative distribution curve (Equation 3), there was a poor correlation between the experimental data and the curve. Graphically, however, the data generally defined a straight line on log-probability paper. A best-fit curve was therefore generated on a computer to fit the data points, $\bar{x}$ and σ being redefined only to provide this best fit. FX and S were designated the two new parameters. This computation is described in Reference 2.

The experimental results are included in Appendix A of this report, Tables A-1 through A-6. GM and GSD are the geometric mean diameter and the standard deviation of the geometric mean, respectively, as defined in Equations 4 and 5. MX is the mass median diameter calculated from the equation and MMD is the experimental mass median diameter. Unlike the frequency data, the mass data did not agree. The mass median diameter could only be predicted to within 8.7μ of the experimental quantity.

3.1.1 Relationship Between Distribution Parameters and the Flow Ratio

A relationship exists between the experimental mass median diameter, x_{mmd}, and the flow-rate ratio of liquid-to-gas for each series of experiments. The results are graphically interpreted in Figures 3, 4, and 5. Included in these figures are the results of the computed mass median diameter MX. The figures, although only within ±8.7μ of the experimental MMD, also show an increase with the flow rate of liquid-to-gas.

There is no significant difference between the results of single and triple injection. This is also true when the second distribution parameter S,* is plotted against the flow-rate ratio (Figures 6, 7, and 8). Both functions are of the type:

$$x_{mmd} = a + b \left(w_l / w_g\right)^c \tag{6}$$

and

$$\sigma = a' + b' \left(w_l / w_g\right)^{c'} \tag{7}$$

where a, b, and a', b' are constants that depend on the physical properties of the liquid, and a and a' also depend on the relative velocity of the gas-to-liquid. That is, at an infinitely small liquid flow rate (analogous to a single droplet exposed to a fast moving gas stream), there is no dependence on flow rate, but only on the intrinsic properties influencing the droplet stability.

*σ will now refer to S, the modified distribution parameter.

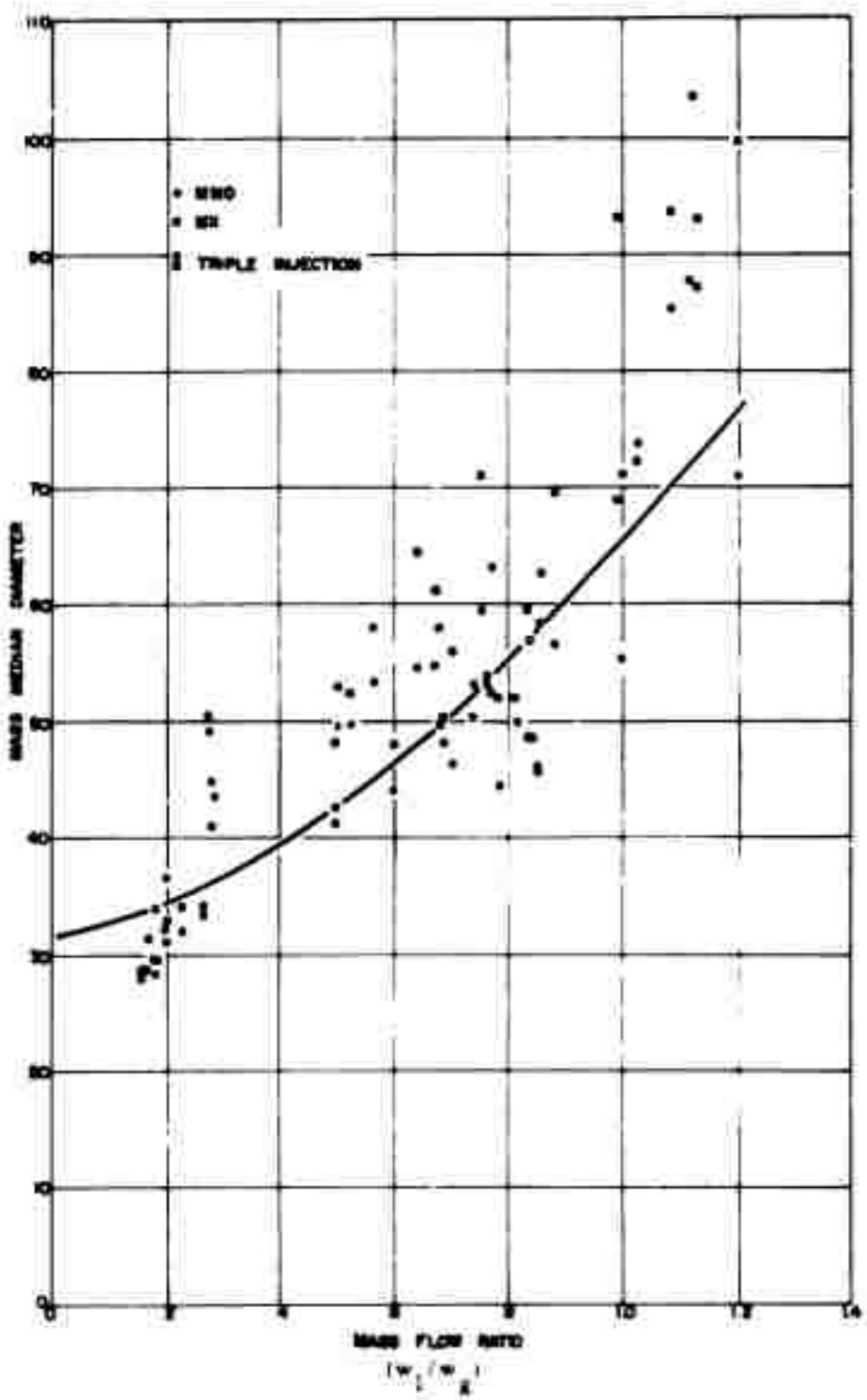

Figure 3. The Atomization of Uvinul-Bis 7° F.

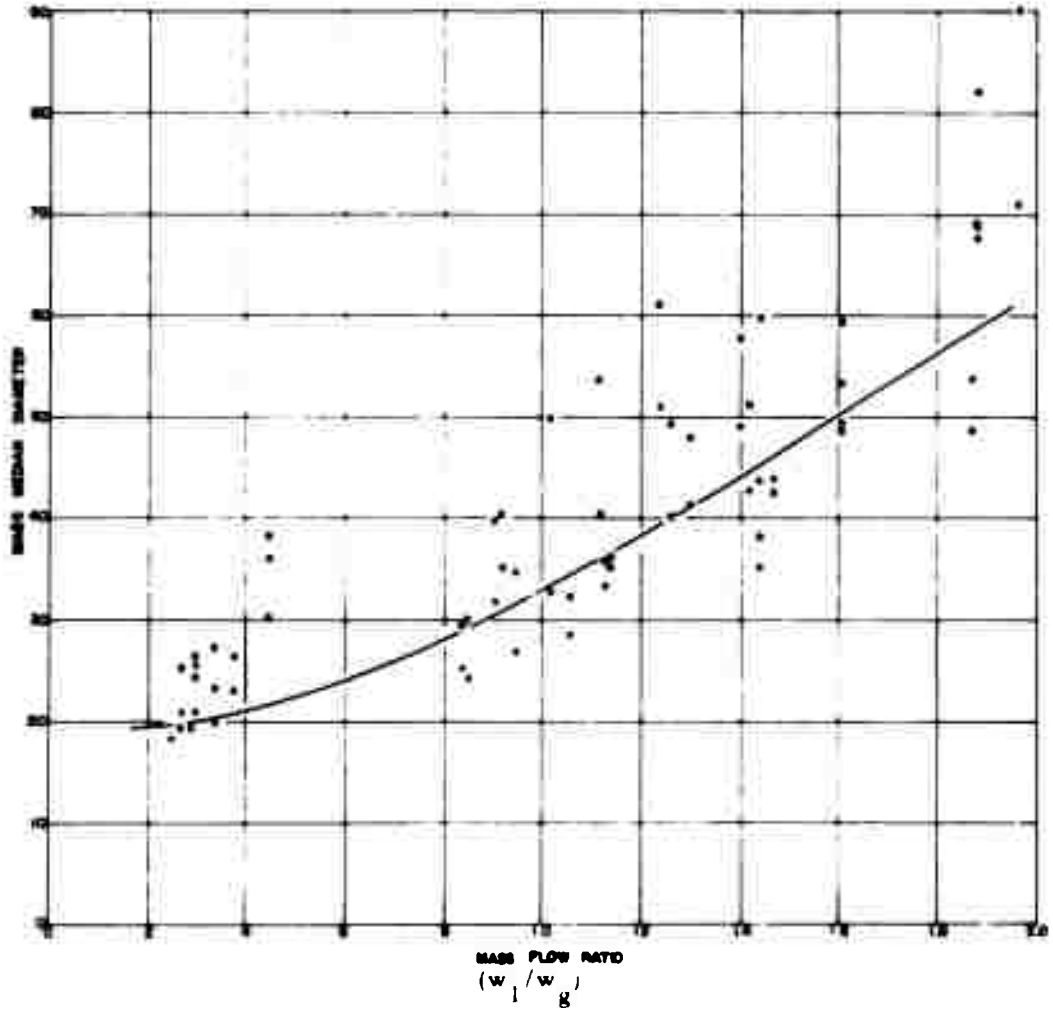

Figure 4. The Atomization of Uvinul-Bis Solution at 833°F.

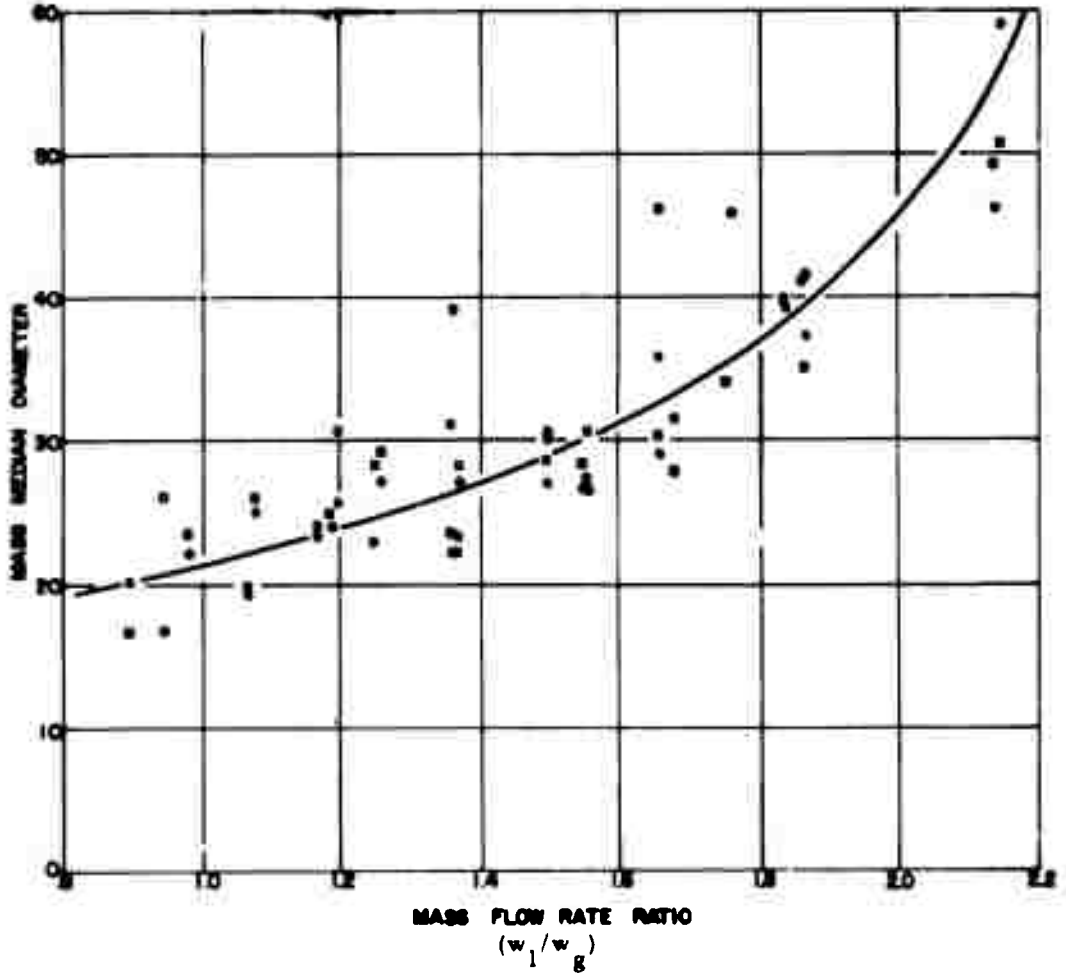

Figure 5. The Atomization of Uvinul-Bis Solution at 1868° F.

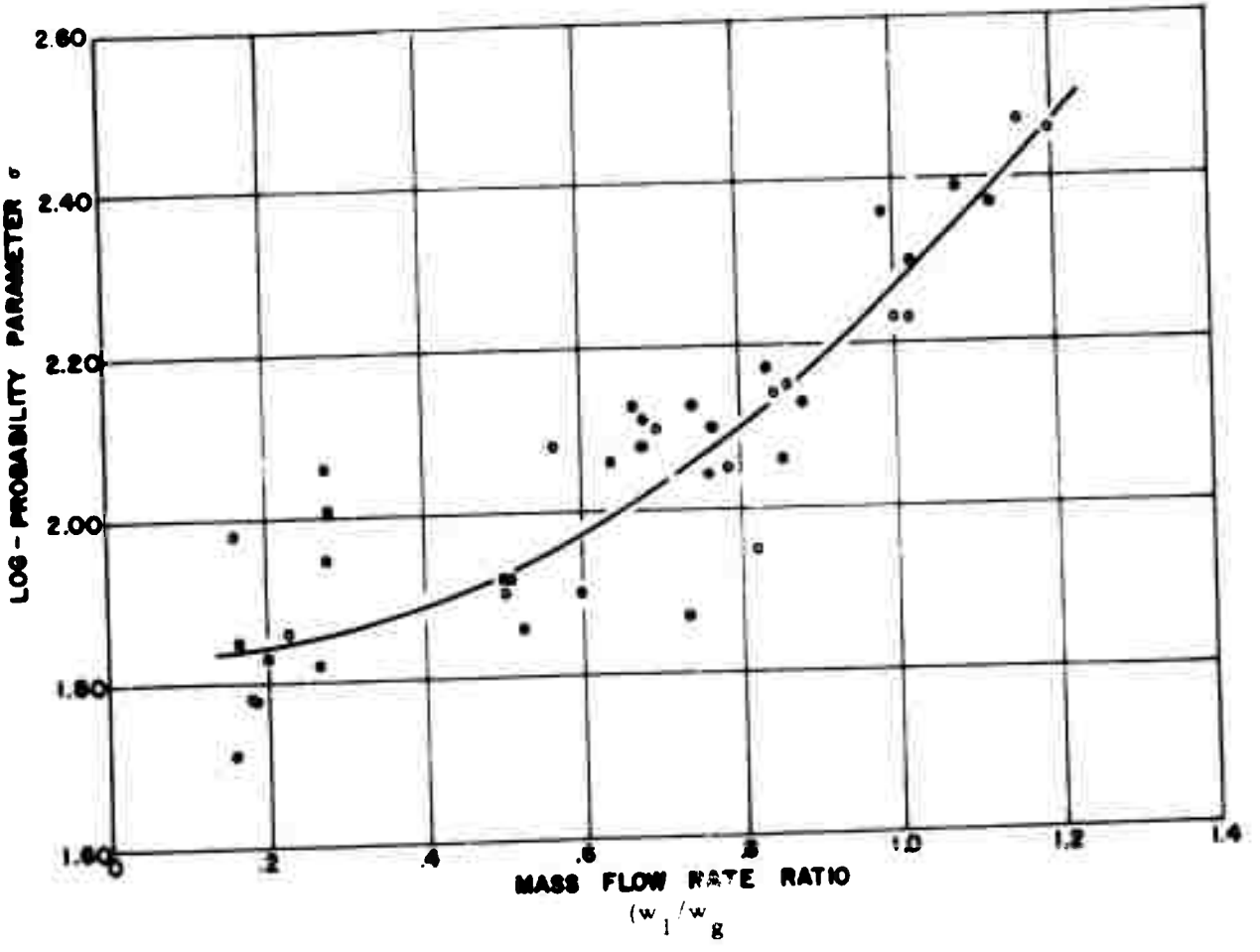

Figure 6. The Atomization of Uvinul-Bis Solution at 7°F.

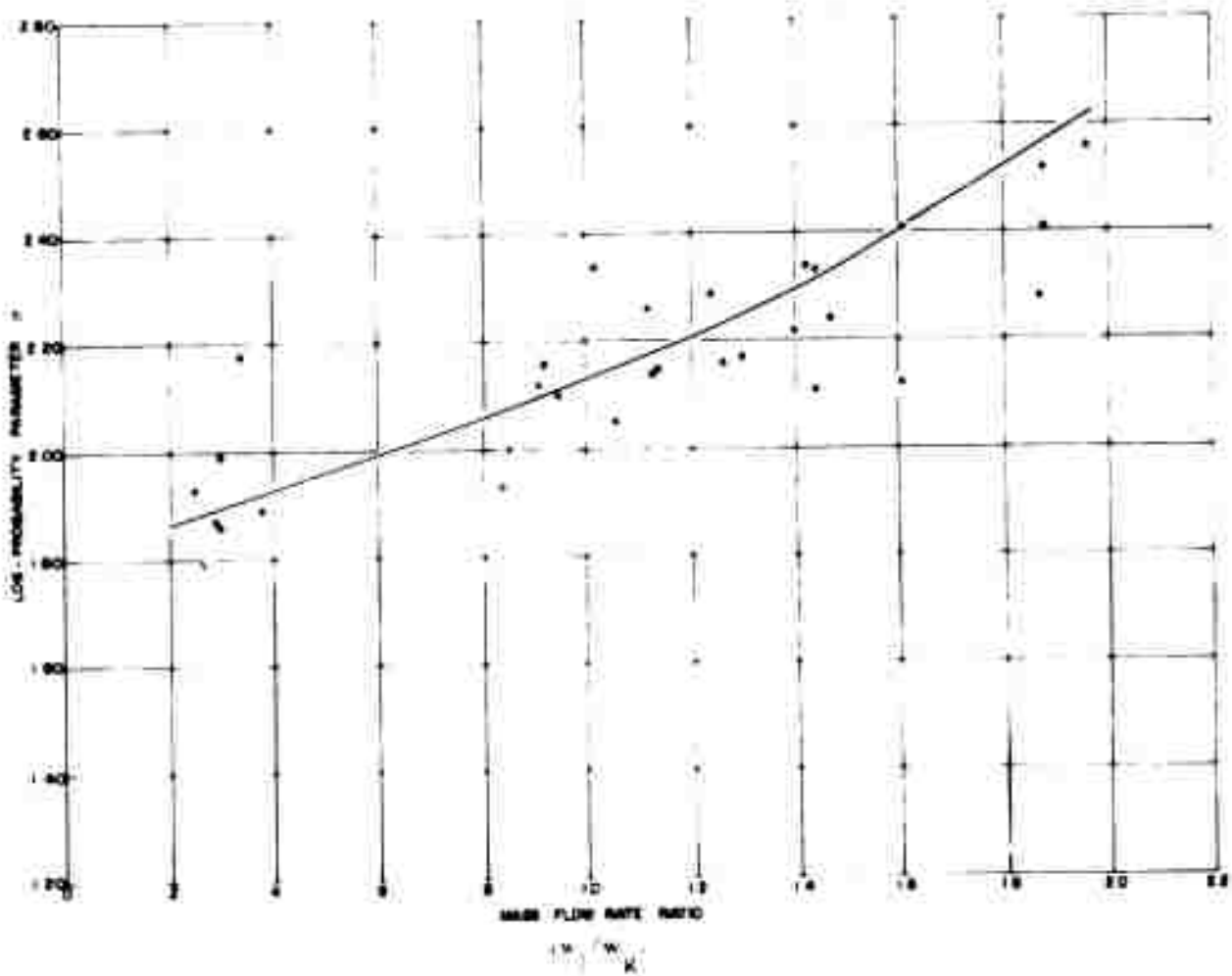

Figure 7. The Atomization of Uranyl Bis Solution at 833°F.

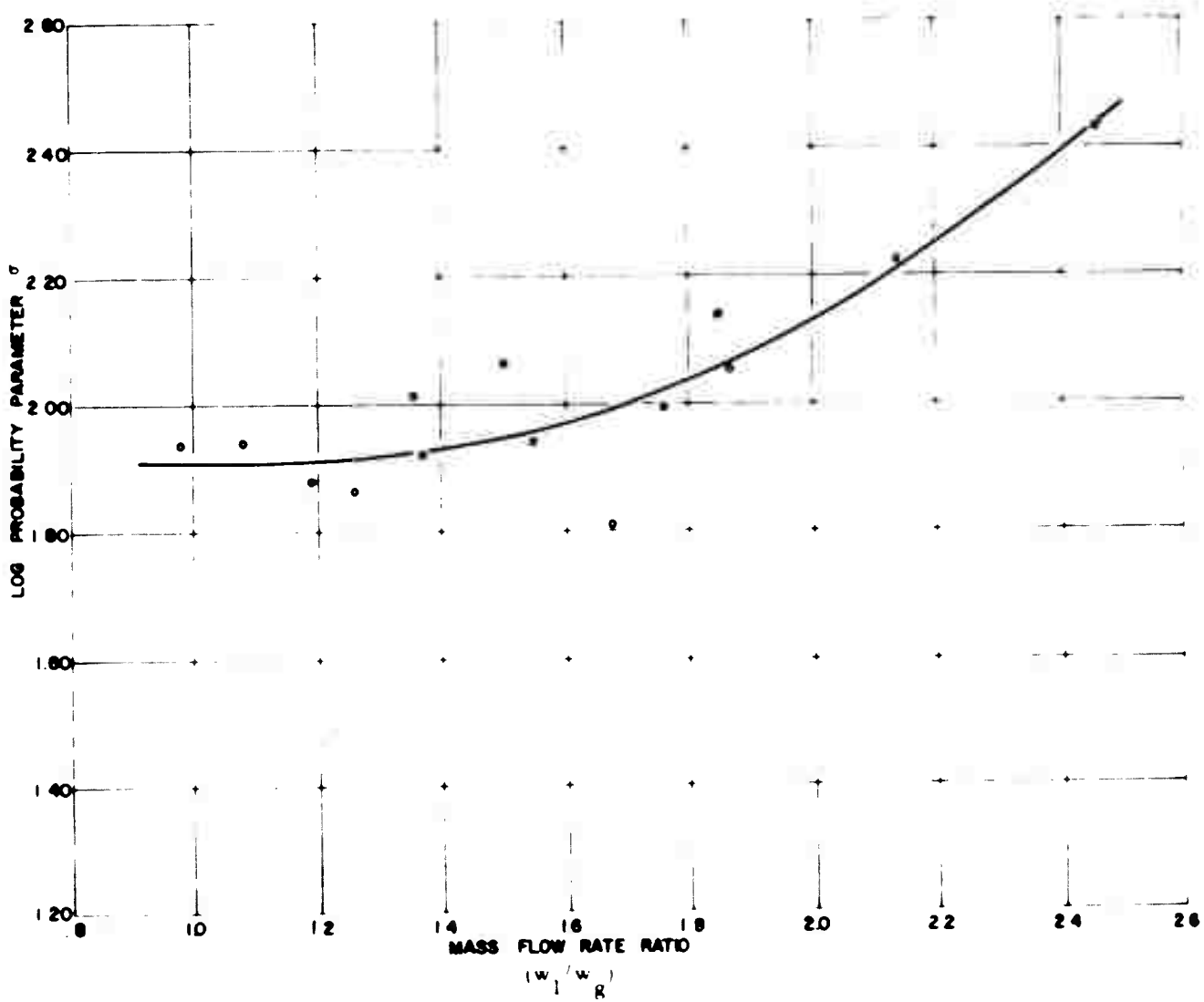

Figure 8. The Atomization of Uvinul Bis at 1868°F

From these two parameters, a complete mass distribution can be derived by inserting them into Equation 3 where $\bar{x} = x_{mmd} = a$, and $\sigma = a'$.

Thus, the distribution that represents the breakup of a single droplet in a fast moving gas stream is

$$Y_m = \frac{1}{\sqrt{2\pi}\,\ln a'} \int_0^{x_1} e^{-\frac{(\ln x_1 - \ln a)^2}{2\ln^2 a'}} \, d\ln x \qquad (8)$$

Y_m = cumulative mass fraction from o to x_1

3.1.2 Relationship between Distribution Parameters and Mean Diameters

Not only can the distributions be reproduced but also various mean diameters may be calculated directly from x_{mmd} and σ. For example,

$$\ln x_{10} = \ln x_{mmd} - 2.5 \ln^2 \sigma \qquad (9)$$

$$\ln x_{20} = \ln x_{mmd} - 2.0 \ln^2 \sigma \qquad (10)$$

$$\ln x_{32} = \ln x_{mmd} - 0.5 \ln^2 \sigma \qquad (11)$$

The Sauter mean diameter, commonly used to describe distributions, is shown in Figures 9, 10, and 11. The data in these figures are calculated from the experimental distributions. The Sauter mean diameter was also calculated from Equation 11 first using x_{mmd} and S and then x_{mx} and S. The largest deviation in a set of data (Tables A-1 through A-6, Appendix A) was ± 2.9 (standard deviation) calculated from x_{mmd}, and ± 5.63 calculated from x_{mx}. These values represent errors of ± 7.5 and 14.3% respectively.

3.2 CORRELATIONS WITH SINGLE DROPLET BREAKUP THEORY

It can be assumed that jet and droplet breakup yield the same size distribution except that in jet breakup there is considerably more coalescence resulting from droplet-droplet impaction. Therefore, the droplet sizes

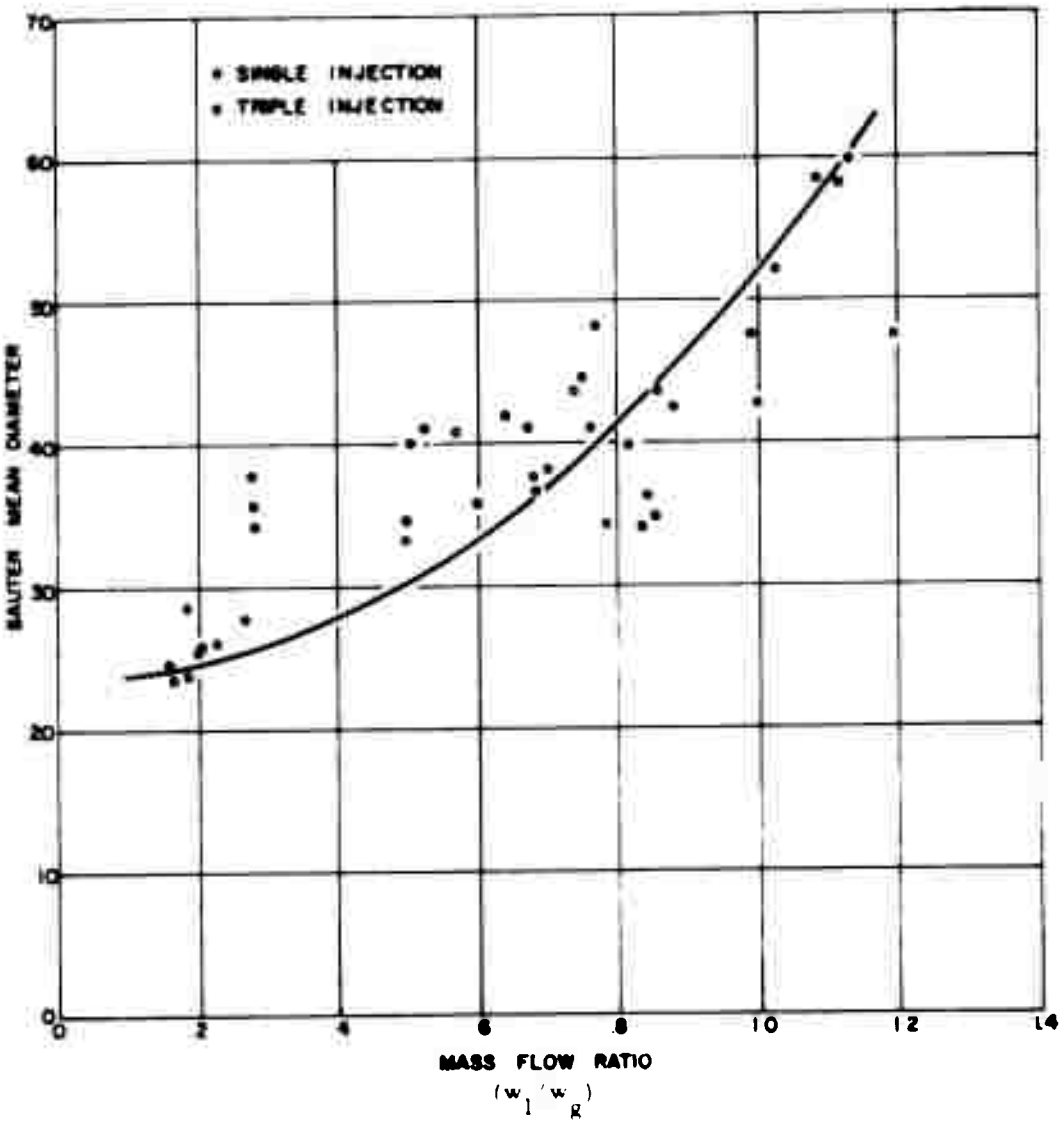

Figure 9. The Atomization of Uvinul-Bis at 7° F.

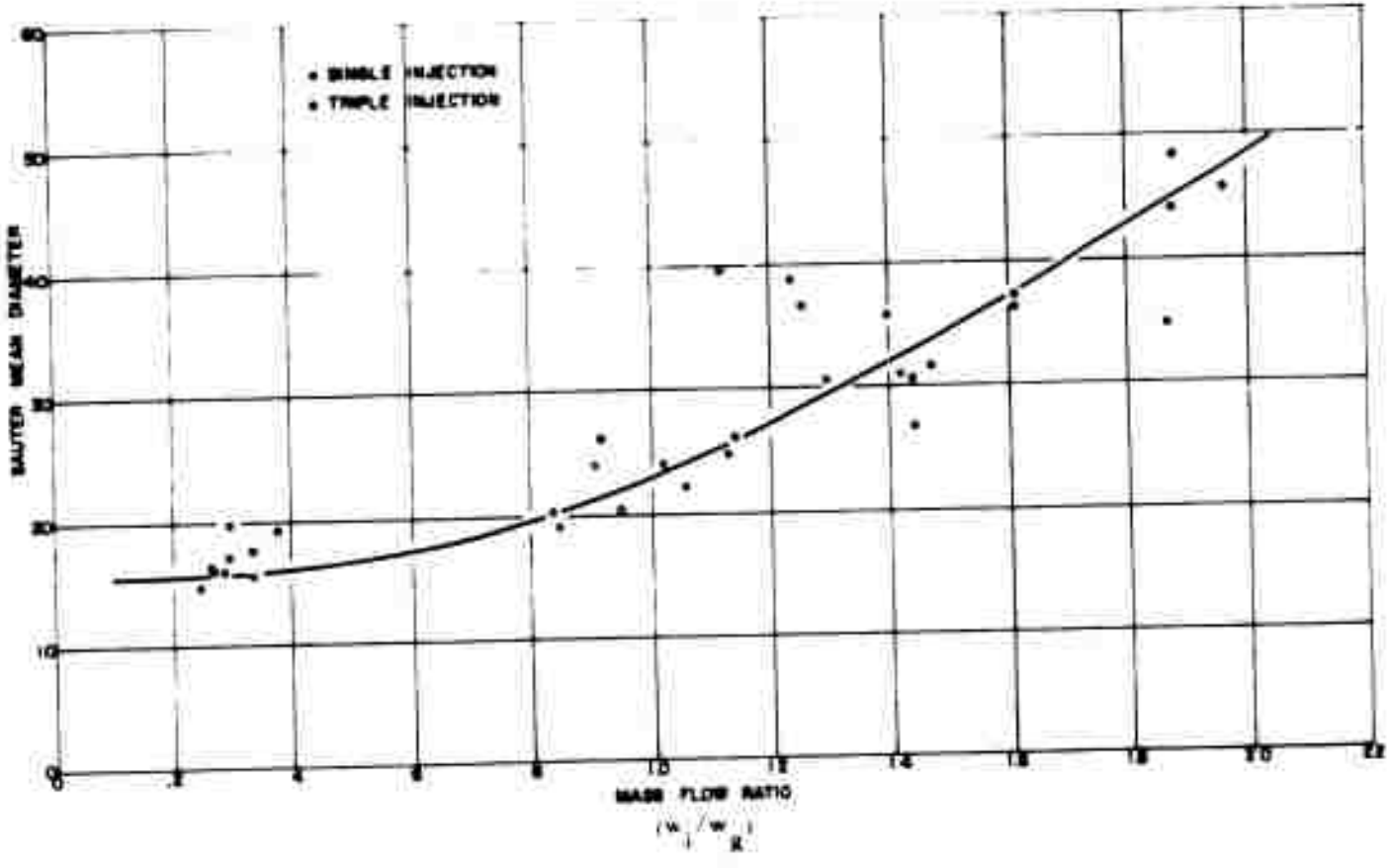

Figure 10. The Atomization of Uvanul-Bis Solution at 833° F.

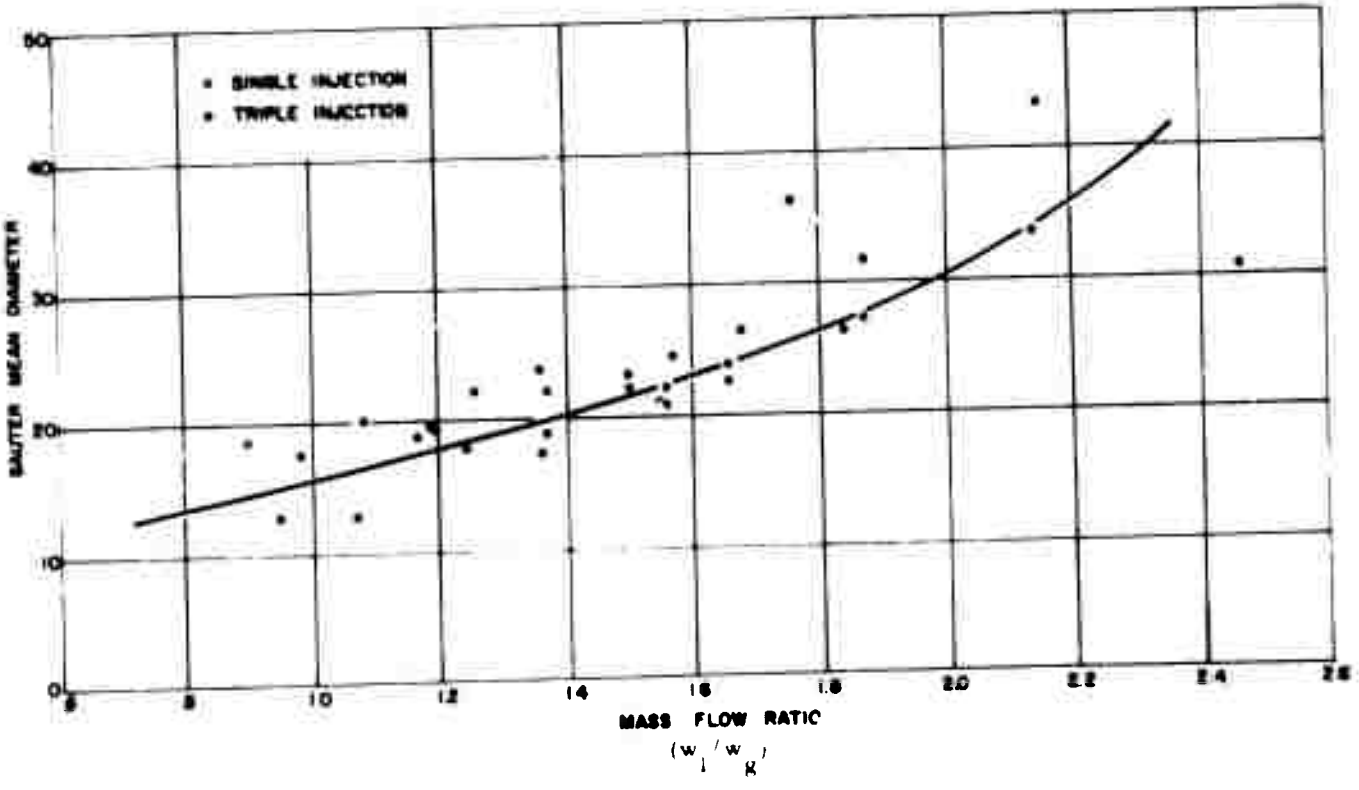

Figure 11 The Atomization of Uranul-Bis Solution at 1868° F.

produced in jet breakup increase as the probability of coalescence or the liquid flow rate increases. The droplet sizes, x, can then be assumed to be an additive quantity:

$$x = a + b\,(w_l/w_g)^c \tag{12}$$

Where a depends upon the same conditions as single droplet breakup, and b on the probability of coalescence and the useful energy transfer, for breakup, from gas stream to liquid. In the Andersen-Wolfe (Reference 5) treatment of droplet breakup, an equation is derived that predicts the mass median diameter. If this equation is solved for the experimental conditions in this study, a droplet size defining an infinitely small w_l/w_g is found.

Andersen-Wolfe Particle-Size Equation:

$$x_{mmd} = \text{mass median diameter} = \left[\frac{136\,\eta_l\,\sigma_l^{3/2}\,D_o^{1/2}}{\rho_a^{2}\,\rho_l^{1/2}\,V^4}\right]^{1/3} \tag{13}$$

where,

η_l = viscosity of liquid, poise $\frac{(\text{dyne-sec})}{\text{cm}^2}$

σ_l = surface tension of liquid dynes/cm

ρ_l = density of liquid, gm/cm^3

D_o = initial drop diameter, assumed to be the injector diameter when a liquid jet is employed, cm

V = relative velocity, cm/sec

136 = dimensional constant (theoretical)

The physical properties of a solution composed of 15% Uvinul-Bis are

η_l = 13.1 centipoise = 0.131 poise

σ_l = 28.6 dynes/cm

ρ_l = $0.959\ \text{gm/cm}^3$

ρ_a = 1.366×10^{-3}

The liquid injector diameter was 0.0686 cm. The relative velocity is 3.285×10^4 cm/sec.

Therefore, the mass median diameter of an aerosol produced when a liquid is injected into an infinitely large gas stream, having the above properties is:

$$x_{mmd} = \left[\frac{136\,(0.131)\,(28.6)^{3/2}\,(0.0686)^{1/2}}{(1.366 \times 10^{-3})^{2}\,(0.959)^{1/2}\,(3.285 \times 10^{4})^{4.4}}\right]^{1/3} \tag{14}$$

$$x_{mmd} = 6.94\,\mu \text{ (mass median diameter)}$$

E. Mayer (Reference 6) derived an expression for the average droplet size obtained on primary atomization. He analytically investigated atomization in high velocity gas streams by considering the behavior of the gas-liquid interface in the regime of capillary wave propagation. With given fluid properties ($\rho_g, \rho_l, \sigma_l, \eta_l$) and relative velocity V, it was shown that all wavelengths exceeding a minimum value will grow at an exponential rate characterized by a time modulus dependent on the wavelength and the fluid parameters. Mayer postulated that when the gas stream-induced wavelength has grown to an amplitude comparable to the minimum wavelength, the crest of the wave is shed as a ligament from which the droplets of diameter x also proportional to the wavelength are formed. The expression is:

$$x = 9\pi\sqrt{3}/16\ B\left(\frac{\eta_l\sqrt{\sigma_l/\rho_l}}{\rho_g V^2}\right)^{2/3} \tag{15}$$

$$= 7.12\ B\left(\frac{\eta_l\sqrt{\sigma_l/\rho_l}}{\rho_g V^2}\right)^{2/3} \tag{16}$$

Calculating, then, the predicted diameter for the atomization of a drop composed of 15% Uvinul-B1s,

$$\frac{x}{B} = 44\mu$$

Assuming $B \sim 0.30$ from Mayer's correlation of Weiss' results (Reference 7)

then $x = 13.2\mu$

Weiss and Worsham experimentally studied the atomization of molten waxes in hot airstreams (Reference 7) The liquid, a molten synthetic wax (Acrawax C, manufactured by Glyco Products Co.) was injected into airstreams having a large cross-section, thus a large mass flow rate when compared to the liquid flow rate. The liquid solidified downstream and the collected solid particles were analyzed by the sedimentation and sieving methods. The results were correlated empirically by a dimensionless equation:

$$\frac{x \rho_a V^2}{\sigma_l} = K \left(\frac{V \eta_l}{\sigma_l} \right)^{2/3} \left(1 + \frac{10^3 \rho_a}{\rho_l} \right) \left(\frac{w_l \rho_l \sigma_l \eta_a}{\eta_l^4} \right)^{1/12} \tag{17}$$

or

$$x = K \frac{(\sigma \eta_l)^{1/3}}{\rho_a V^4} \left(1 + \frac{10^3 \rho_a}{\rho_l} \right) \left(\frac{w_l \rho_l \sigma_l \eta_a}{\eta_l^4} \right)^{1/12} \tag{18}$$

where η_a is the viscosity of the gas, and w_l is the mass flow rate of liquid. K is an experimental constant equal to 0.61

Taking the data from Tables A-1 and A-2, Appendix A, in which the liquid flow rate was 1.05 gm/sec, and plotting against w_l/w_g gives Curve 1 in Figure 12. From Weiss' equation, a mass median diameter of 20μ is obtained when the relative velocity is 3.285×10^4 cm/sec If Curve 1 is extrapolated, it appears that a value of 20μ is approached

Although the data in Tables A-3 and A-4, Appendix A, and Figures 2 and 5 are the results of atomization experiments in which the initial gas temperature was 833°F, a careful evaluation of the equilibrium gas-liquid temperature showed that the equilibrium temperature was close to 75°C, assuming at least a 70% heat transfer efficiency:

$$w_l / w_g = C_{p_g} (T_1 - T_2) / C_{p_l} (T_2 - T_A) \tag{19}$$

The properties of the 15% Uvinul-Bis solution are illustrated in Figures A-1, A-2, and A-3, Appendix A Under these conditions, the mass median diameter calculated is 11.3μ and an extrapolation of Curve 2 results in a close comparison.

BLANK PAGE

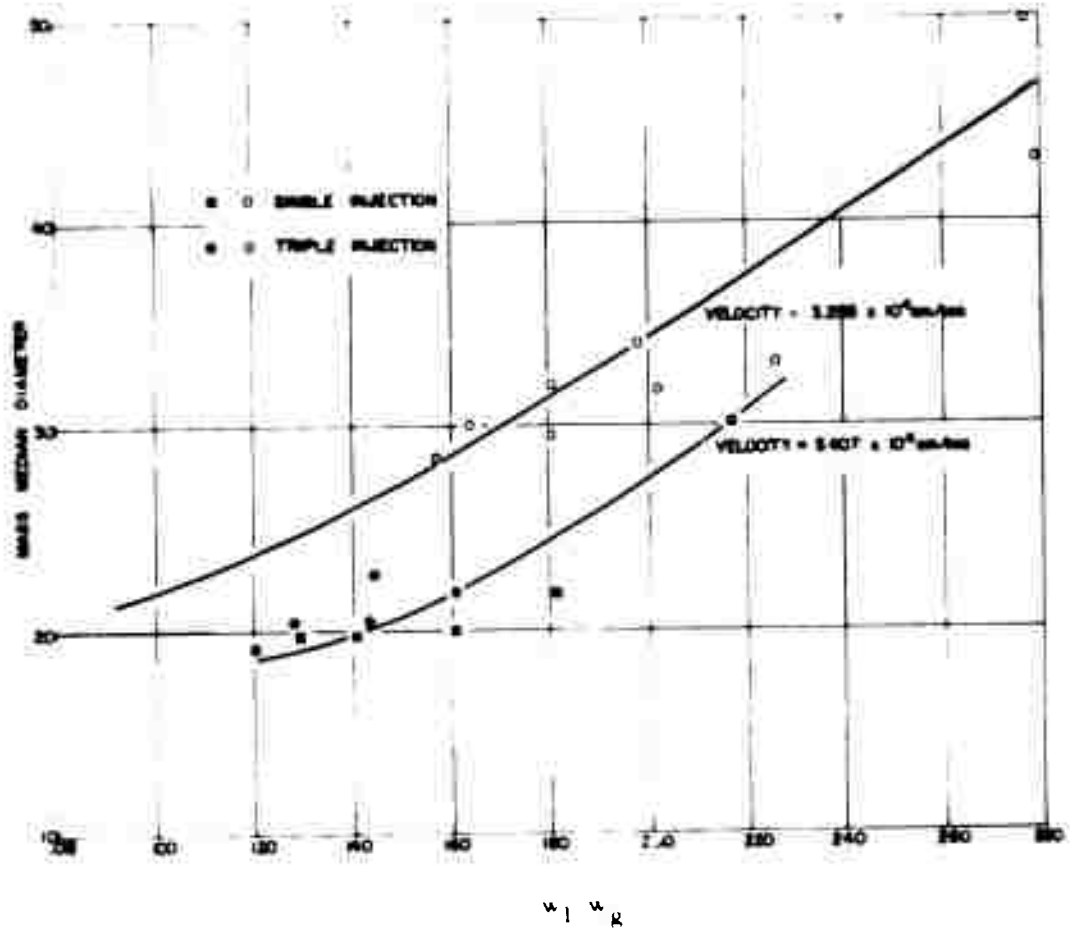

Figure 12 Correlation of Atomization Experiments at 7° F and 833° F with the Weiss Worsham Equation, Liquid Injection Rate 1.05 gm/sec.

The Andersen-Wolfe equation appears to qualitatively agree with the experimental results if the results of either set of data in Figure 13 is predicted from the other by

$$x \quad x_2 = \frac{\eta_1 \sigma_1^{1.2}}{P_a^2 \rho_1^{1/2} V^{4.5}} \text{ condition 1} \Big/ \frac{\eta_1 \sigma_1^{1.2}}{P_a^2 \rho_1^{1/2} V^{4.5}} \text{ condition 2}$$

1.53 (21)

The comparison, showing smaller particles produced when the gas temperature reached 833 F, indicates that vaporization took place, further reducing the droplet sizes

3.3 CORRELATIONS WITH OTHER ATOMIZATION STUDIES

Nukiyama and Tanasawa (Reference 8) investigated the relationship between the fineness of mist generated from small airblast atomizers and the operating variables and physical properties of the liquid or solution. These results are embodied in the empirical formula

$$D_{32} \quad \frac{585\sqrt{\sigma}}{V\sqrt{\rho}} + 597 \left(\frac{\eta}{\sqrt{\sigma\rho}}\right)^{0.45} \left(\frac{1000 Q_l}{Q_g}\right)^{1.5} \qquad (21)$$

Bitron (Reference 9) carried out further studies on airblast atomizers having divergent air channels where air could exceed sonic velocities. Bitron's work thus suggests that the N-T equations, although developed from experimentation at subsonic velocities, can be extended to sonic and supersonic velocities.

The first term in Equation 21 is similar to equations by Andersen-Wolfe and Mayer, therefore concluding that $585\ \sigma/V\sqrt{\rho}$ describes a mean droplet size for single droplet breakup. For the conditions at 7 F it also predicts a quantity close to that of Andersen-Wolfe and Mayer. It must be noted that the latter two equations predict a mass median diameter whereas the N-T equation predicts the Sauter mean diameter. Generally, the difference between the two is small $D_{32} \quad D_{mmd}$. They are all consistent in showing a dependence of D on:

$$\sim \sigma^{1/2} \text{ to } \sigma^{1.3},\ V^{-4/3} \text{ to } V^{-1},\ \rho_l^{-1/6} \text{ to } \rho_l^{-1/2}$$

BLANK PAGE

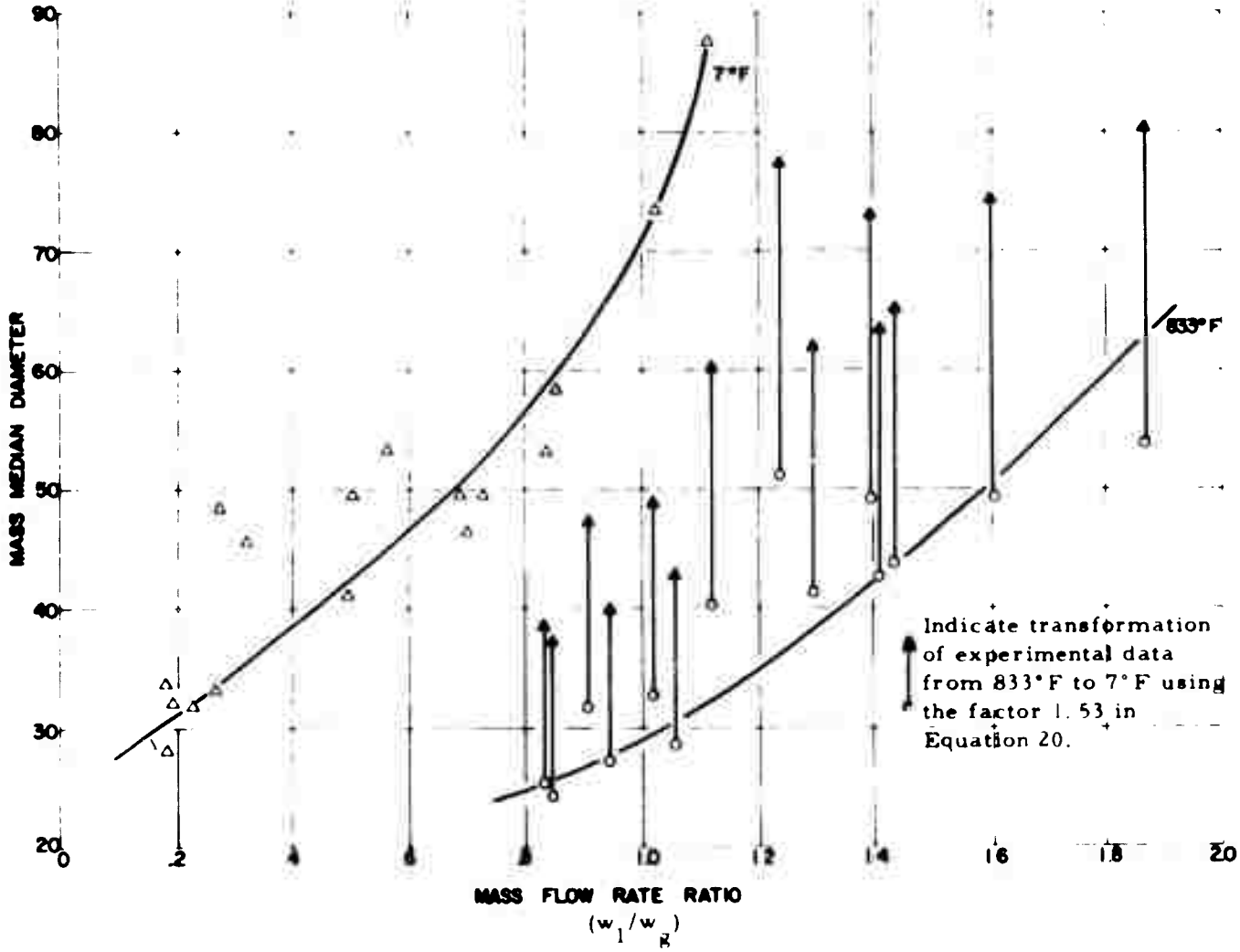

Figure 13. Correlation of Atomization Experiments at 7° and 833°F With the Andersen-Wolfe Equation

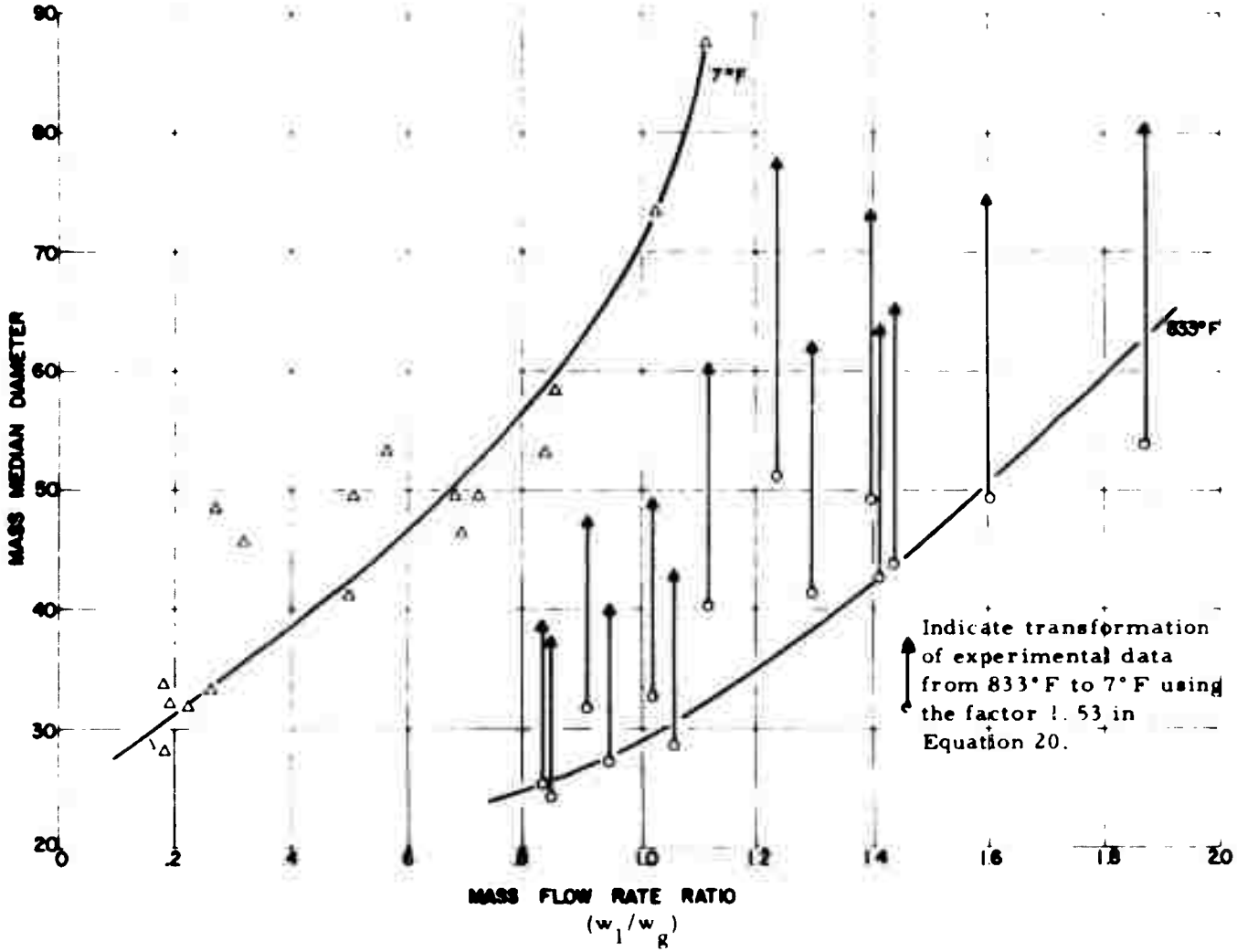

Figure 13. Correlation of Atomization Experiments at 7° and 833°F With the Andersen-Wolfe Equation

The results of atomizing the solution of 15% Uvinul-bis at various temperatures in terms of the Sauter mean diameter appear in Figure 14 The results of the atomization experiments at 7°F are shown with the predicted curve derived from the N-T equation in Figure 15 The correlation, although not too good, is similar to that obtained by Gordon (References 10 and 12) and N-T showing large difference in the region where Q_l/Q_g becomes small

Equations of the form,

$$x_{mmd} = a + b\,(Q_l/Q_g \times 10^3)^c \qquad (22)$$

and

$$\sigma = a' + b'\,(Q_l/Q_g \times 10^3)^{c'} \qquad (23)$$

were found for the cold-gas atomization results These equations resemble the Nukiyama-Tanasawa equation, in which the Sauter mean diameter, x_{32} can be predicted

The equations were

$$x_{mmd} = 3\ 19 + 49\ 4\,(Q_l/Q_g \times 10^3)^{1\ 63} \qquad (24)$$

$$x_{mmd} = 31\ 9 + 33\ 0\,(w_l/w_g)^{1\ 59} \qquad (25)$$

$$\sigma = 1\ 85 + 0\ 69\,(Q_l/Q_g \times 10^3)^{1\ 51}, \text{ and} \qquad (26)$$

$$\sigma = 1\ 86 + 0\ 41\,(w_l/w_g)^{1\ 50} \qquad (27)$$

Similar equations for the atomization experiment at 833°F were also determined They are:

$$x_{mmd} = 17\ 9 + 46\ 8\,(Q_l/Q_g \times 10^3)^{1\ 49} \qquad (28)$$

$$x_{mmd} = 17\ 5 + 16\ 1\,(w_l/w_g)^{1\ 49} \qquad (29)$$

$$\sigma = 1\ 83 + 0\ 43\,(Q_l/Q_g \times 10^3)^{1\ 49} \qquad (30)$$

$$\sigma = 1\ 83 + 0\ 33\,(w_l/w_g)^{1\ 50} \qquad (31)$$

BLANK PAGE

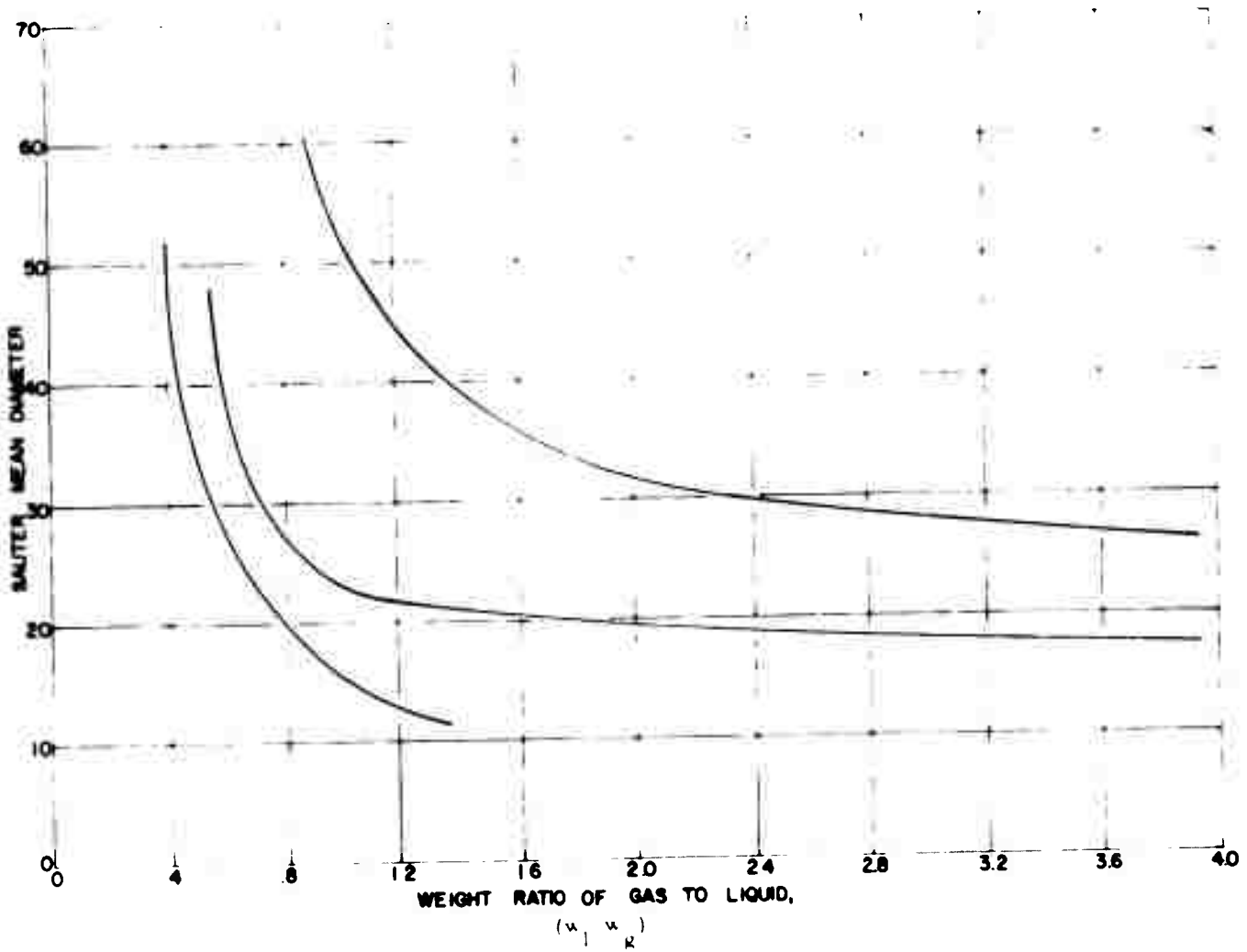

Figure 14 Atomization of Uvinul-Bis at Three Temperatures

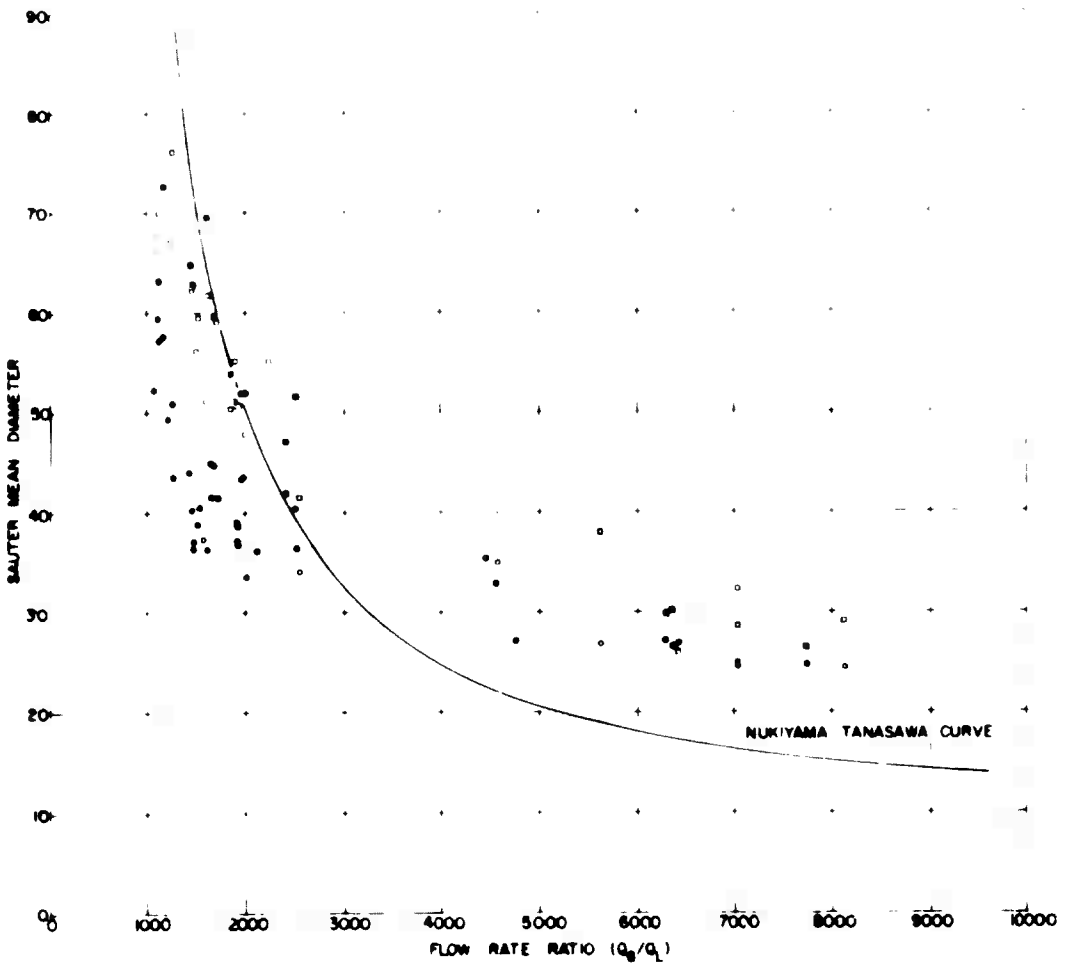

Figure 15. Cold-Gas Atomization of a Solution of 15% 2,4-Dihydroxylbenzophenone - 85% bi -(2-Ethylhexyl) Hydr gen Phosphite Comparison of Results with the Nukiyama-Tanasawa Equation

Equations, of a similar form, were determined relating the Sauter mean diameter and flow rate ratios from these studies of Uvinul-Bis and those of Gordon (Reference 12) for the atomization of pure Bis They are,

$$x_{32} \quad 10\ 6 + 56\ 6\ (Q_l/Q_g \times 10^3)^{0\ 91} \quad \text{(Bis) (Reference 12)} \qquad (32)$$

$$x_{32} \quad 24\ 8 + 28\ 2\ (Q_l\ Q_g \times 10^3)^{1\ 37} \quad \text{Bis-Uvinul)} \qquad (33)$$

No overall conclusions can be made regarding these equations as to the influence of physical properties, flow rate conditions, or relative velocity because of the limitations of the properties investigated It is important to note, however, that the values of (c) in Equations 24 through 31 correspond closely to 1 5, the value found in the Nuk.yama-Tanasawa equation

Figure 16 shows the difference in the Sauter mean diameter due to the viscosity of the liquid The results of Aerojet experiments at 1868°F are compared with the atomization of di-isooctylphthalate and bis (2-ethylhexyl) hydrogen phosphite in air by investigators at SRI (Reference 11) Upon extrapolation (as w_l/w_g becomes small*) the dependency of the Sauter mean diameter upon viscosity is approximately $x_{32}\ \eta^{5/3}$ assuming a constant viscosity ratio with temperature

3 4 FINE AEROSOL DROPLETS

As the gas flow and temperature increase, the fraction of fine droplets left suspended in the aerosol chamber increases These droplets were not included in the size distributions, but were treated separately The results of this analysis appear in Figures 17 through 20 and are summarized in Figures 21 and 22 These curves show the same type of trend as those describing particle-size distribution An additional experimental series at 1382°F, appears in Figure 19 Particle-size data were not obtained for this series

*When w_l/w_g becomes small the thermal energy used to vaporize the liquid becomes small

BLANK PAGE

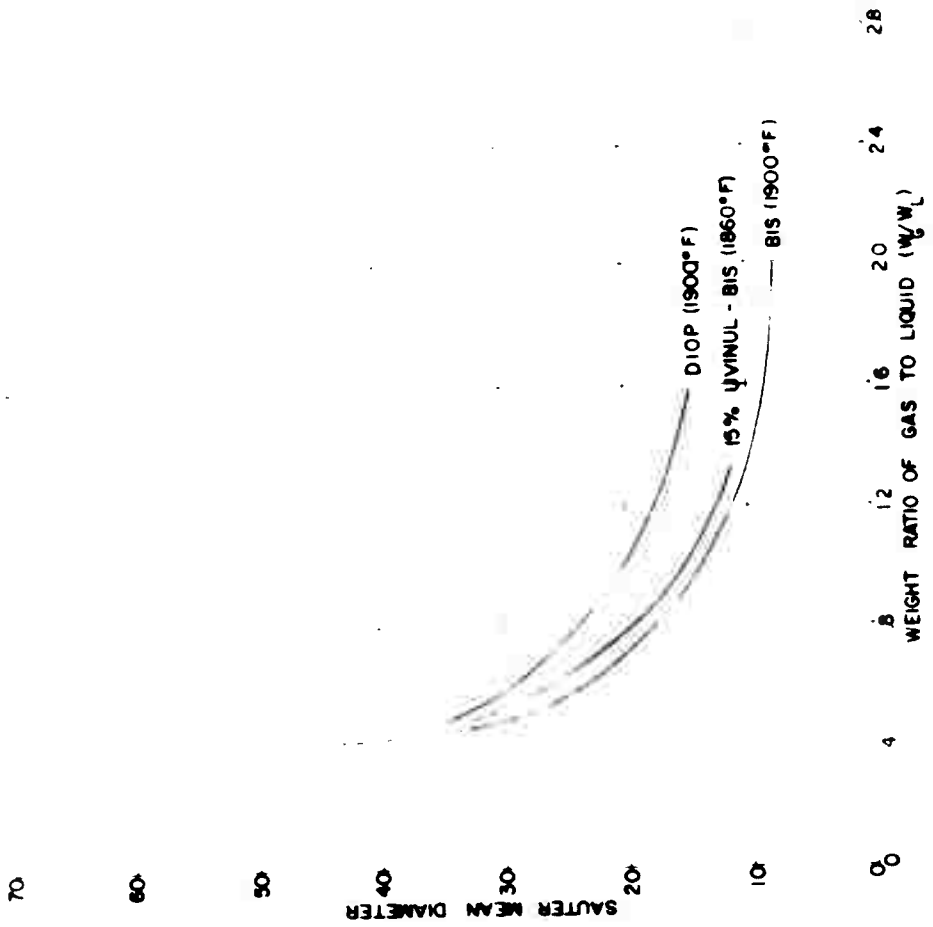

Figure 16. Influence of Viscosity on Particle Size.

	Viscosity cpoise	Density gm/cm^3	Surface Energy dynes/cm
DIOP	63.4	0.982	32
15% Uvinul-Bis	13.1	0.961	28.7
Bis	6.1	0.927	29.7

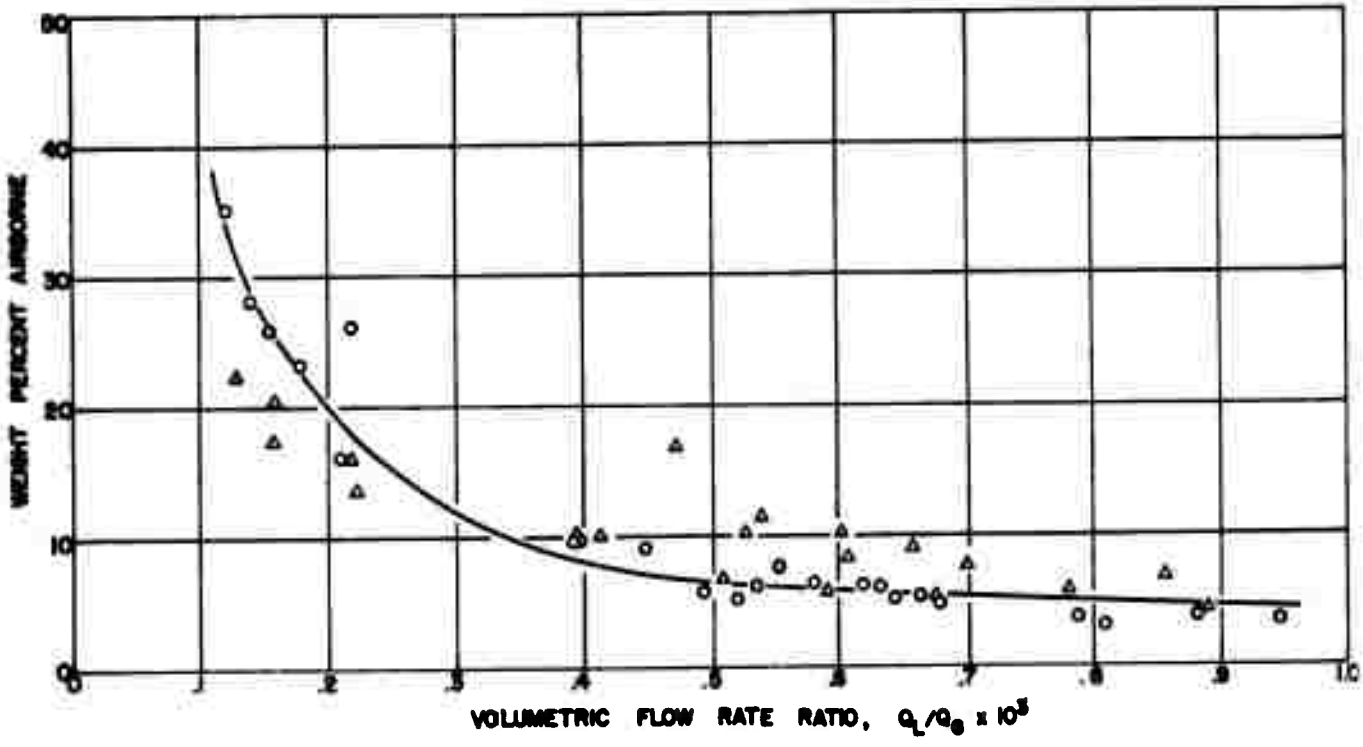

Figure 17. Percent Airborne vs Volumetric Flow Rate Ratio Mass Airborne Represents Droplets less Than 7 Microns (Diameter) Gas Temperature 7°F.

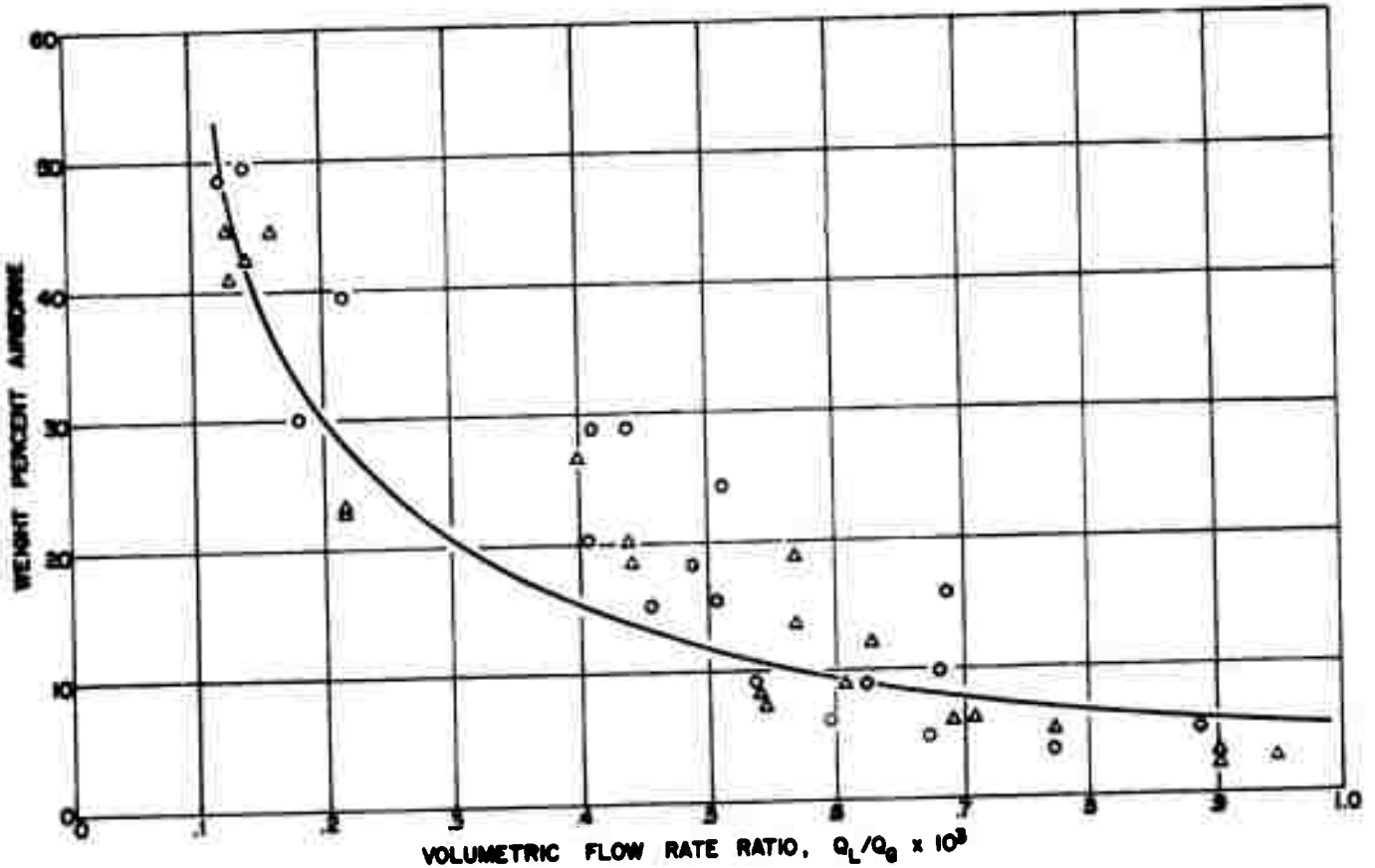

Figure 18. Percent Airborne vs Volumetric Flow Rate Ratio Mass Airborne Represents Droplets less Than 7 Microns (Diameter) Gas Temperature 833°F.

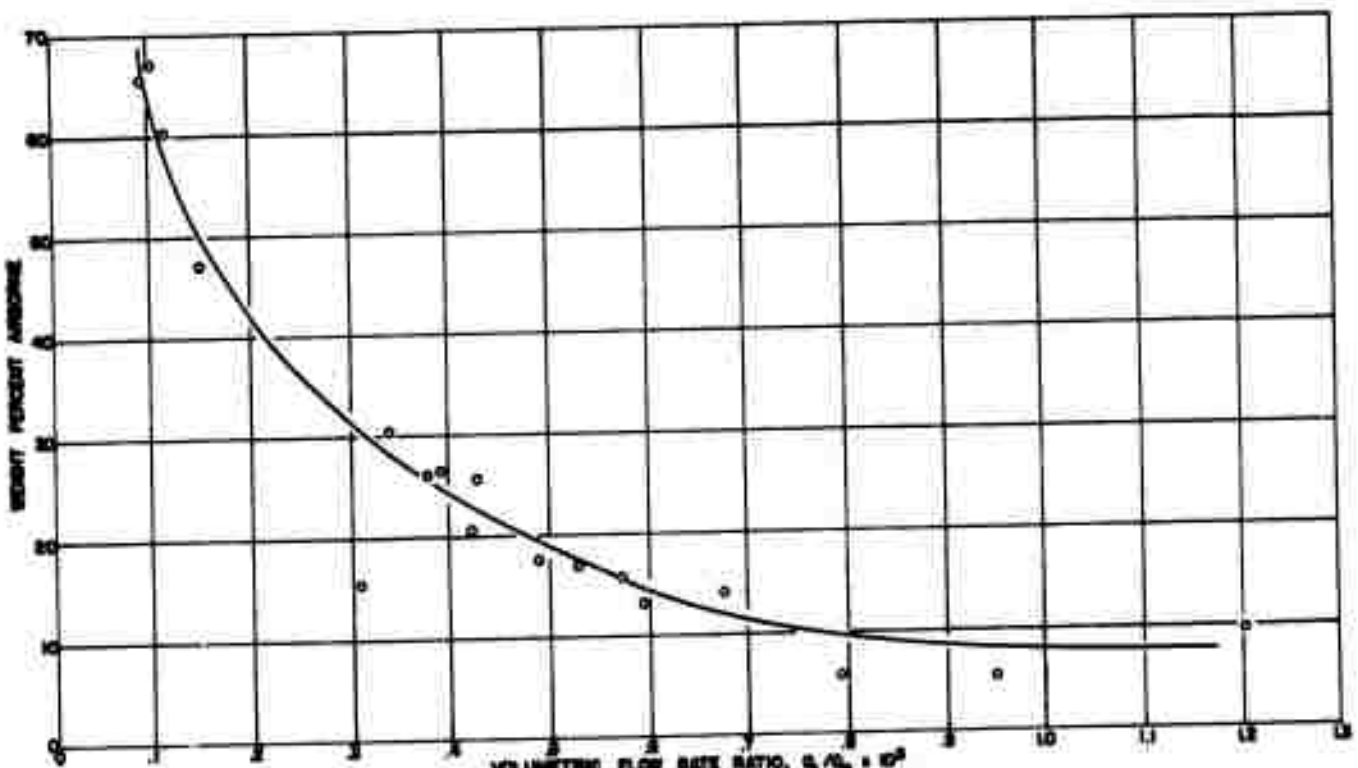

Figure 19. Percent Airborne vs Volumetric Flow Rate Ratio Mass Airborne Represents Droplets less Than 7 Microns (Diameter) Gas Temperature 1383°F.

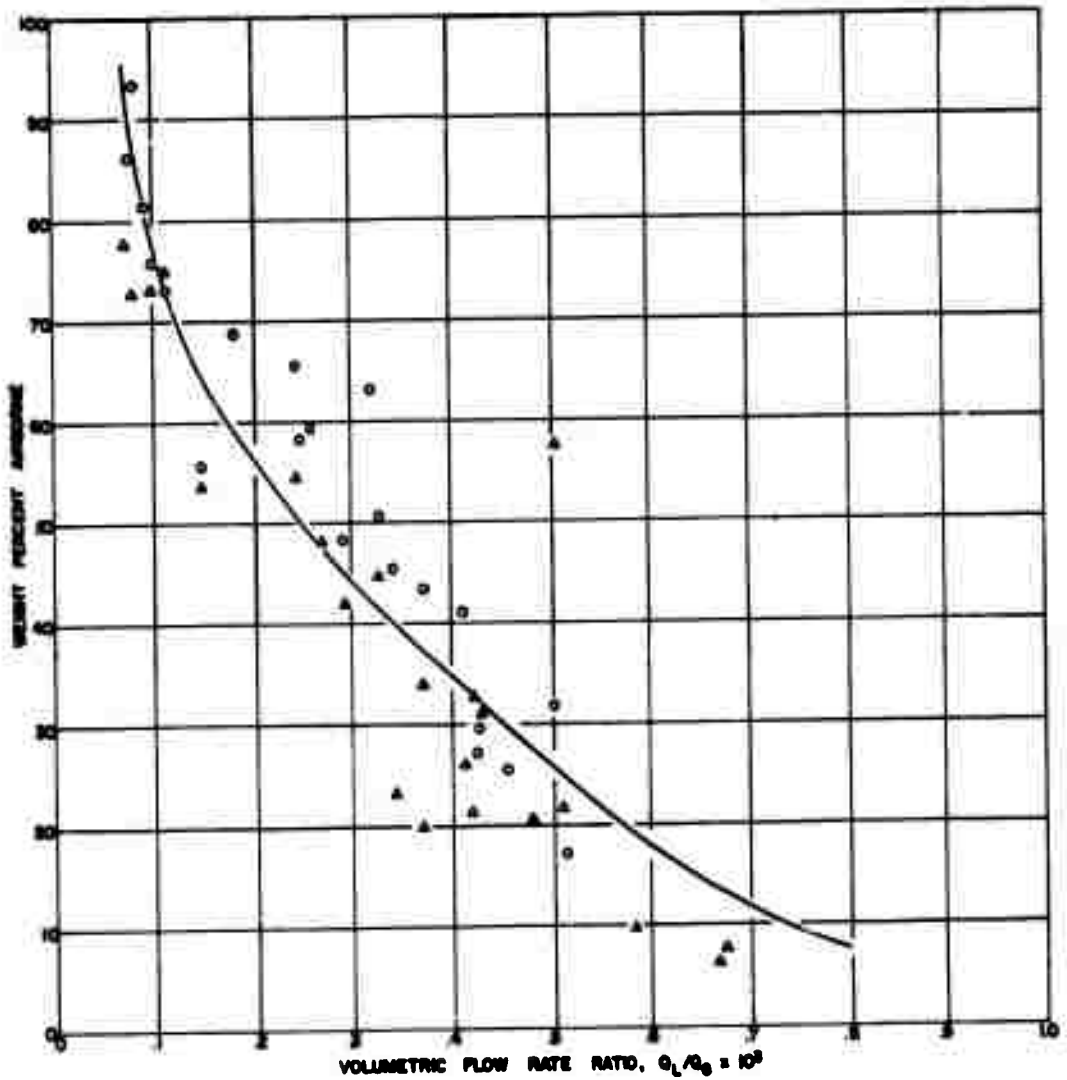

Figure 20. Percent Airborne vs Volumetric Flow Rate Ratio Mass Airborne Represents Droplets less Than 7 Microns (Diameter) Gas Temperature 1868°F.

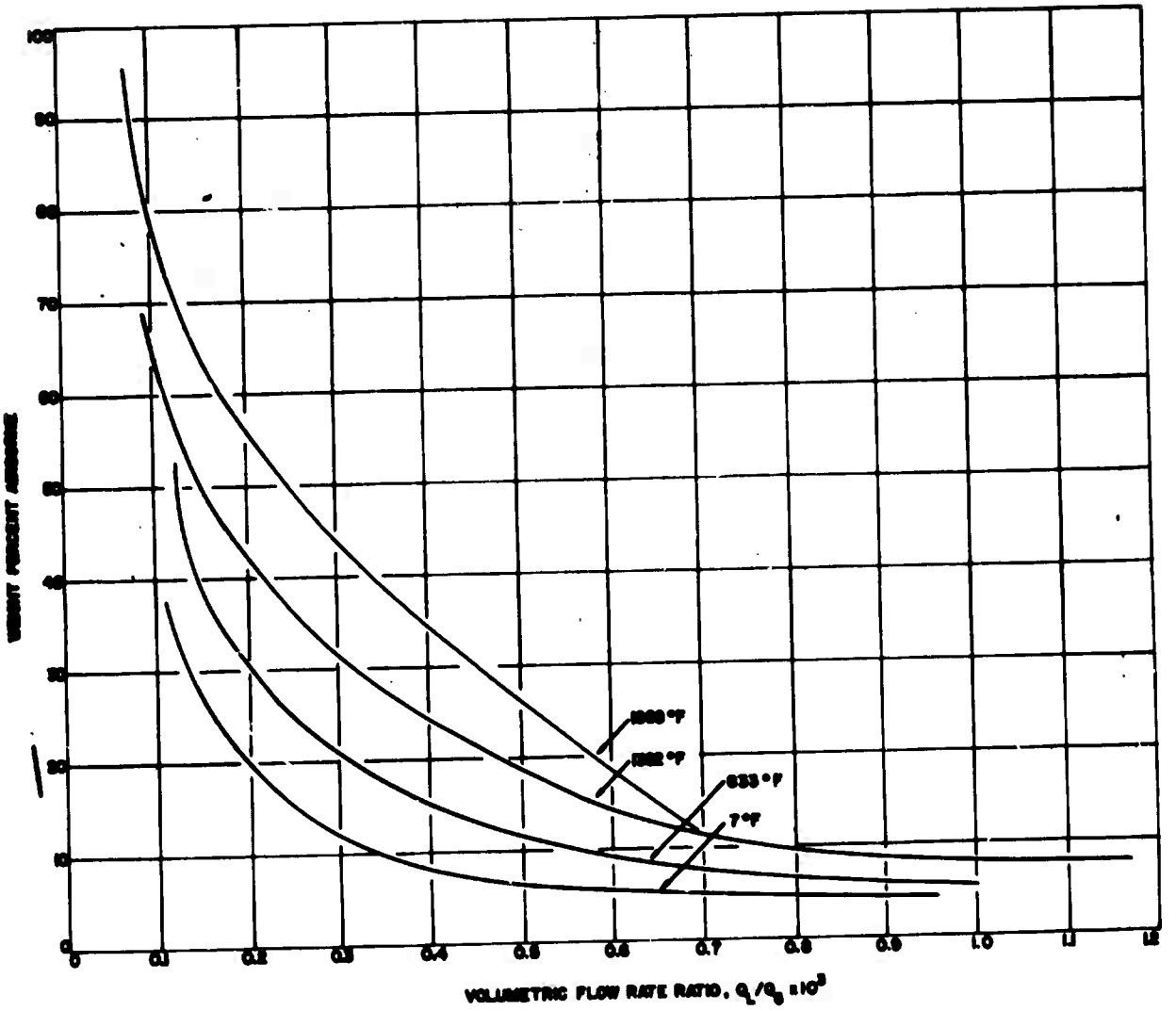

Figure 21. Percent Airborne vs Volumetric Flow Rate Ratio.

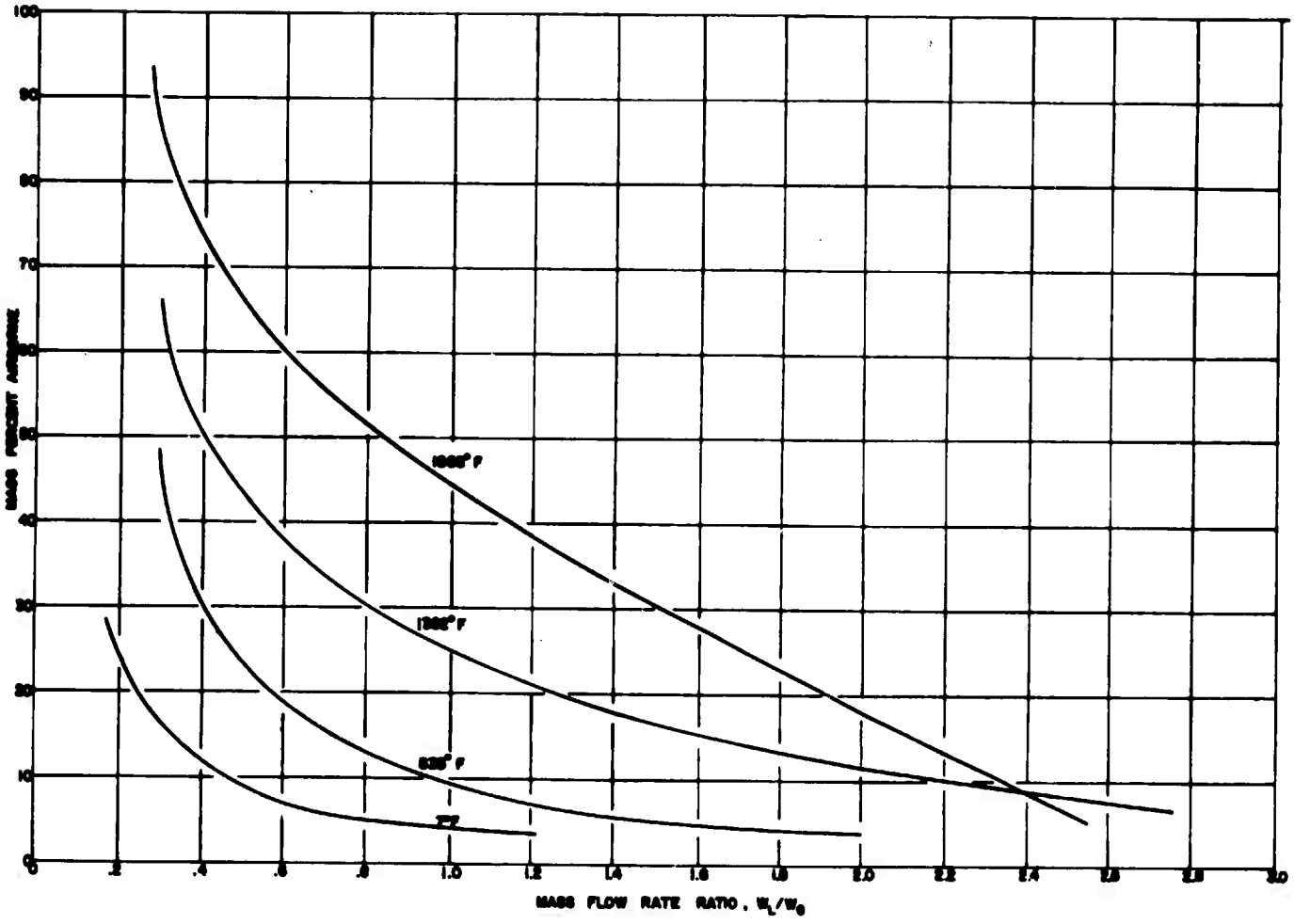

Figure 22. Percent Airborne vs Mass Flow Rate Ratio.

4. CONCLUSIONS AND RECOMMENDATIONS

Specific relationships for the atomization of a solution composed of 15% 2, 4-dihydroxybenzophenone in 85% bis(2-ethylhexyl) hydrogen phosphite, by weight, can be made between the flow rate ratio of gas-to-solution and the modified parameters of the logarithm-probability distribution function. The suggested relationship between these parameters and the flow rate ratio are

$$x = a + b(w_l/w_g)^c \tag{34}$$

and

$$\sigma = a' + b'(w_l/w_g)^{c'} \tag{35}$$

By inserting these two equations into the log-probability distribution function, a method is obtained for determining the cumulative distribution resulting from the atomization of a liquid or solution with given physical properties

$$Y = \frac{1}{\sqrt{2\pi}\,\ln\left[a' + b'(w_l/w_g)^{c'}\right]} \int_0^{x_i} e^{\frac{-(\ln x_i - \ln\left[a + b(w_l/w_g)^c\right])^2}{2\ln^2\left[a' + b'(w_l/w_g)^{c'}\right]}} d\ln x \tag{36}$$

a is defined as the mass median diameter expected for single droplet breakup and can be described by the derived functions of either Wolfe-Andersen or Mayer. Figure 23 shows the variation of the mass median diameter with relative velocity as reported by Wolfe and Andersen for pure bis. The experimental points show good correlation with their theory, indicated by the curve in this figure. There also appears to be a relationship between σ and the relative velocity for this same experiment (Figure 24). It is suggested therefore that a' is a function of the relative velocity and other physical properties, probably the same as those which define a.

BLANK PAGE

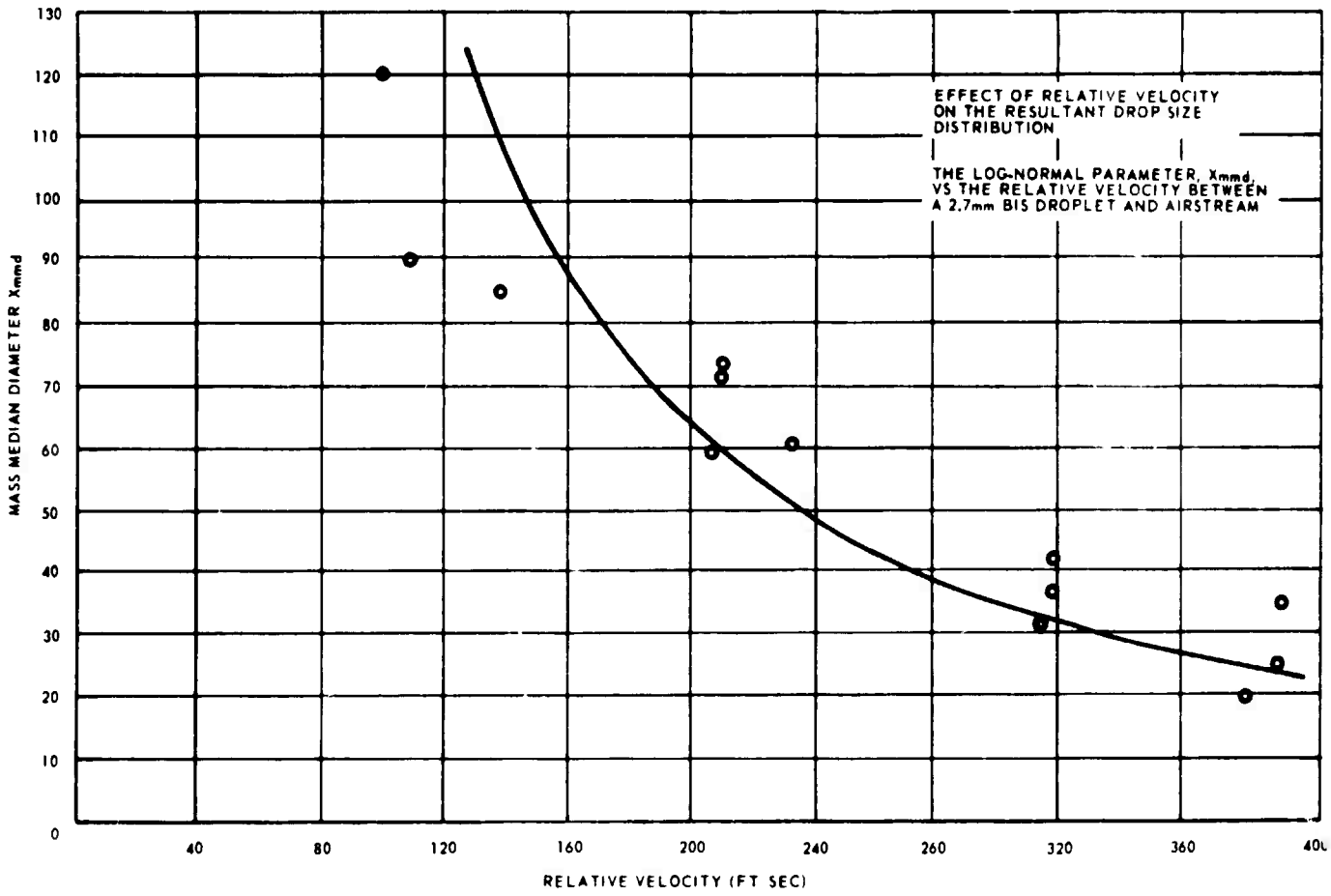

Figure 23. Wolfe-Andersen Variation of the Mass Median Diameter With Relative Velocity.

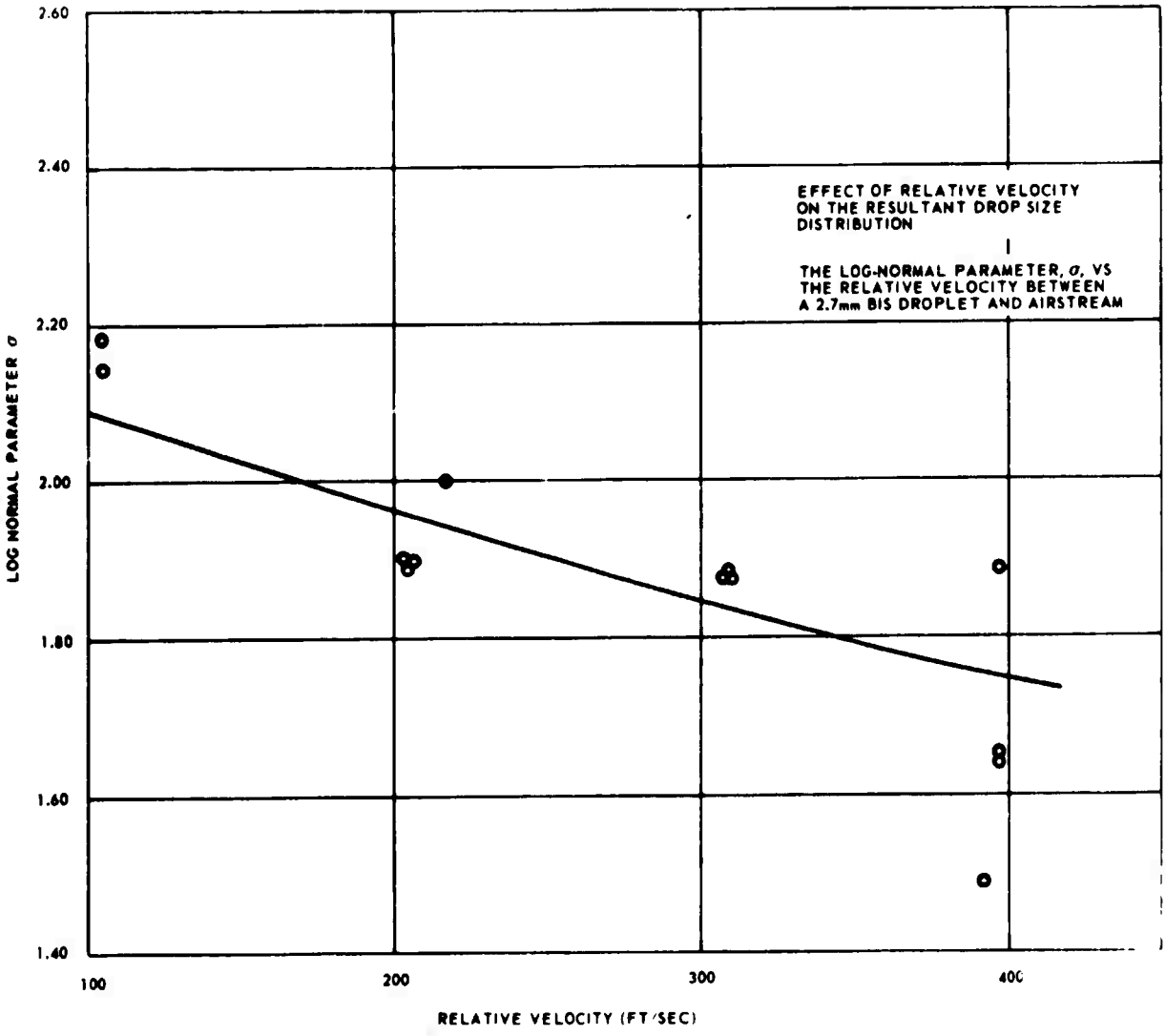

Figure 24. Relationship Between σ and the Relative Velocity for the Wolfe-Andersen Experiment.

From the results of this study c and c' seem to be constant and very close to 1.5 as found by Nukiyama and Tanasawa. Undetermined are the factors b and b' which should be similarly defined as the second term in the Nukiyama-Tanasawa equation.

For single droplet breakup the term

$$b(w_l/w_g)^c$$

and

$$b'(w_l/w_g)^c$$

become insignificant as compared to a and a', respectively. Therefore, the cumulative distribution for single droplet breakup becomes

$$Y = \frac{1}{\sqrt{2\pi}\ln a'} \int_o^{x_i} e^{\frac{-(\ln x_i - \ln a)^2}{2\ln^2 a'}} d\ln x \qquad (37)$$

The mass fraction of aerosol below 7 microns, unconsidered in the droplet-size distribution treatment, is also shown to be a function of the flow rate ratio. In the experiments atomized by nitrogen at 7°F the mass median diameter was determined of 90% or more of the particles when the mass flow ratio, w_l/w_g was $\geq .4$. In the experiments at 833°F, 90% or more of the mass was considered at mass flow rate ratios ≥ 1.0. In each of these experiments therefore the true mass median diameter is slightly lower than that found. It would be expected that the a term will be lowered thus resulting in a closer correlation of the mass median diameter with that predicted by Wolfe-Andersen and Mayer.

A comparison of results between this investigation and those conducted by Nukiyama-Tanasawa* generally agrees.

It is recommended that in future studies an attempt be made to relate the surface tension. viscosity, density, and relative velocity to the resultant droplet-size distribution by use of the suggested distribution parameters. Also methods of including the entire size range produced in the analyses should be determined.

*Nukiyama-Tanasawa considered droplets greater than 10 microns.

REFERENCES

1. Karp, G. S., and G. P. Wachtell, "Fundamental Investigations of the Breakup of Viscoelastic Fluid Jets," Franklin Institute Final Report F-AZ 118, p. 8-11, March 1961.

2. Brown, R. E., and K. Leonard, "Methods of Describing Droplet-Size Distributions from Atomized Solutions," Aerojet-General Corporation Special Report 0395-04(14)SP, February 1964.

3. Sass, S., and J. Cassidy, Anal. Chem. 28,1968 (1956).

4. O'Donovan, P. A., and F. Martin "Analytical Method for Uvinul-400 (2, 4-Dihydroxybenzophenone)" Aerojet-General Corporation Report 1311-63(02)ER, October 1963.

5. Wolfe, H. E., and W. H. Andersen, "Kinetics, Mechanisms, and Resultant Droplet Sizes of the Aerodynamic Breakup of Liquid Drops," Aerojet-General Corporation Special Report 0395-04(18)SP, February 1964.

6. Mayer, E. ARS Journal 31, 1783 (1961).

7. Weiss, M. A., and C. H. Worsham ARS Journal 29, 252 (1959).

8. Nukiyama, S., and Y. Tanasawa, Trans. Soc. Mech. Eng. (Japan) 4 (1938), 5 (1939), 6 (1940). Translated by E. Hope, Defense Research Board (Canada) 1950.

9. Bitron, M. D., Ind. Eng Chem. 47, 23 (1955).

10. Gordon, M., "Cold-Gas Atomization of Low Volatility Liquids," U. S. Army Chemical CWLR 2333 (January 1960).

11. Gordon, M., "Hot-Gas Aerosolization of Liquids of Low Volatility," U. S. Army CRDLR 3030 (September 1960).

12. Gordon M., Factors Affecting Atomization of Liquids with Cold Gas.

13. "Factors Determining the Particle-Size of Aerosols Generated by Hot-Gas Atomization," Southern Research Institute, Final Report 4180-890-XIII, September 1959.

APPENDIX A

Table A-1. Atomization at 70°F, Single Injector.

QL/QG	WL/WG	GM	FX	GSD	S	MX	MMD
0.218×10^{-3}	0.277	10.66	10.40	2.00	2.06	50.59	49.36
0.156	0.198	9.47	9.31	1.93	1.96	36.61	32.15
0.178	0.226	10.87	10.68	1.82	1.86	34.04	31.98
0.142	0.181	11.13	10.97	1.81	1.78	29.89	33.98
0.123	0.157	11.63	11.78	1.73	1.71	28.09	28.62
0.142	0.181	10.77	10.73	1.83	1.78	29.62	28.16
0.210	0.267	11.48	11.48	1.80	1.82	34.22	33.35
0.399	0.506	14.58	14.53	1.99	1.92	53.12	49.69
0.448	0.568	11.82	11.55	2.04	2.08	58.29	53.32
0.645	0.818	13.25	13.49	1.93	1.95	51.99	49.86
0.581	0.736	14.86	15.44	1.85	1.87	50.40	53.14
0.394	0.500	12.43	12.40	1.89	1.90	42.81	41.07
0.537	0.680	10.92	10.69	2.03	2.11	58.14	49.66
0.882	1.116	10.08	9.03	2.09	2.47	105.54	87.60
0.664	0.842	10.13	9.91	2.08	2.14	57.19	48.49
0.810	1.026	9.74	8.97	2.07	2.30	72.47	73.78
0.620	0.785	11.14	11.06	2.04	2.05	52.03	44.42
0.679	0.860	10.85	10.67	2.08	2.15	62.79	58.42
0.789	1.000	10.49	10.13	2.08	2.23	71.26	55.17
0.552	0.699	10.81	10.73	2.06	2.10	56.09	46.29
0.945	1.195	9.60	8.79	2.12	2.46	99.98	70.94

Table A-2. Atomization at 7°F, Triple Injector.

QL/QG	WL/WG	GM	FX	GSD	S	MX	MMD
0.219×10^{-3}	0.279	10.71	10.64	1.87	1.95	41.05	44.98
0.223	0.284	10.04	9.88	1.88	2.01	43.48	43.48
0.159	0.202	11.07	10.87	1.87	1.83	32.87	31.03
0.129	0.164	9.95	9.95	1.94	1.85	31.50	28.67
0.696	0.881	12.36	12.24	2.09	2.13	69.44	56.68
0.591	0.747	12.86	12.76	2.08	2.13	71.17	59.42
0.506	0.640	13.40	13.42	2.10	2.06	64.63	54.63
0.472	0.599	13.86	13.69	1.91	1.90	47.93	44.04
0.414	0.525	16.29	16.29	1.89	1.86	52.38	49.87
0.395	0.500	13.11	13.25	2.07	1.92	48.12	42.75
0.674	0.855	9.93	9.58	1.98	2.06	46.07	45.58
0.856	1.086	10.45	9.59	2.09	2.39	93.73	85.43
0.539	0.683	10.39	10.01	2.02	2.08	50.29	48.07
0.608	0.770	10.31	9.84	1.97	2.10	52.34	63.23
0.527	0.668	11.24	10.99	2.08	2.13	61.16	54.84
0.890	1.128	10.65	9.78	2.06	2.37	93.15	87.21
0.603	0.763	11.96	11.69	2.04	2.04	53.90	53.16
0.781	0.989	10.55	10.12	2.17	2.36	93.33	68.96
0.659	0.836	10.10	9.79	2.14	2.17	59.62	48.85

Table A-3. Atomization at 833°F, Triple Injector.

QL/QG	WL/WG	GM	FX	GSD	S	MX	MMD
0.902×10^{-3}	1.88	7.46	6.19	2.00	2.52	82.16	67.81
0.902	1.88	7.75	6.69	1.98	2.41	69.22	68.88
0.948	1.96	7.60	6.36	2.07	2.56	90.24	70.99
0.774	1.61	6.89	5.77	1.97	2.41	59.31	53.24
0.708	1.47	6.92	5.97	1.90	2.24	42.53	43.80
0.692	1.44	7.60	7.03	1.89	2.11	38.17	35.26
0.608	1.26	7.58	6.77	1.87	2.16	40.17	49.31
0.548	1.14	6.93	6.17	1.88	2.15	36.06	35.09
0.541	1.13	6.93	6.30	1.90	2.14	35.88	33.30
0.634	1.35						
0.571	1.19						
0.571	1.19						
0.442	0.92	7.85	6.48	1.76	2.18	40.43	35.21
0.439	0.91						
0.401	0.84						
0.216	0.45	7.10	5.52	1.71	2.22	37.88	36.36
0.216	0.45	6.54	4.42	1.66	2.41	45.54	37.38
0.216	0.45						
0.162	0.34	4.31	4.34	2.18	2.18	27.30	23.86
0.144	0.30	6.16	6.32	2.16	1.99	26.51	25.45
0.143	0.30	7.44	7.60	2.11	1.86	24.36	21.00
0.128	0.27	4.93	5.11	2.21	2.07	25.33	21.00

Table A-4. Atomization at 833°F, Single Injector.

QL/QG	WL/WG	GM	FX	GSD	S	MX	MMD
0.888×10^{-3}	1.87	6.62	6.34	2.10	2.28	48.79	53.71
0.774	1.61	8.61	8.81	2.00	2.12	48.58	49.47
0.674	1.40	8.30	8.46	2.17	2.22	57.86	49.17
0.597	1.24	7.86	7.66	2.12	2.29	61.20	51.16
0.539	1.12	6.79	7.21	2.19	2.26	53.82	40.50
0.488	1.02	5.39	5.60	2.43	2.34	49.97	32.89
0.689	1.44	7.62	6.93	2.08	2.33	59.97	43.86
0.684	1.42	6.84	5.83	1.95	2.34	51.42	42.63
0.625	1.30	8.35	7.75	2.04	2.17	47.79	41.46
0.509	1.06	7.36	6.86	1.92	2.05	32.31	28.85
0.455	0.95	7.16	6.65	2.00	2.10	34.73	27.00
0.439	0.91	7.50	7.05	2.02	2.12	39.07	31.87
0.411	0.85	7.49	7.09	2.00	2.00	30.12	24.36
0.407	0.84	8.27	7.98	1.98	1,93	29.51	25.34
0.217	0.45	4.10	4.89	2.62	2.30	47.39	30.42
0.182	0.38	7.55	7.75	2.15	1.89	26.44	23.60
0.161	0.34	4.83	4.93	2.14	2.05	23.42	20.03
0.141	0.29	6.11	6.27	2.04	1.87	20.55	19.45
0.129	0.27	6.76	6.93	1.99	1.79	19.39	19.49
0.122	0.25	5.12	5.40	2.15	1.93	19.77	18.47

Table A-5. Atomization at 1868°F, Single Injector.

QL/QG	WL/WG	GM	FX	GSD	S	MX	MMD
0.411×10^{-3}	1.50	8.75	8.85	1.93	1.86	28.54	27.15
0.374	1.37	7.17	7.95	2.05	1.91	28.38	27.35
0.372	1.36	6.70	6.98	2.31	2.13	39.18	31.68
0.343	1.25	5.99	6.13	1.92	2.04	28.37	23.06
0.455	1.66	4.27	3.91	2.20	2.47	46.20	35.93
0.513	1.87	6.43	6.25	2.00	2.21	41.52	37.43
0.455	1.66	6.35	6.48	1.95	2.04	30.35	29.15
0.590	2.15	6.16	5.83	2.12	2.33	50.79	59.01
0.426	1.56	7.24	7.47	2.21	1.98	30.58	26.54
0.259	0.946	4.69	4.84	2.22	2.11	26.11	16.97
0.426	1.56	7.13	7.56	2.04	1.93	27.51	27.46
0.247	0.901	9.32	10.13	1.53	1.50	16.76	20.15
0.291	1.07	7.69	6.40	1.97	2.47	19.64	19.35
0.321	1.17	5.32	5.36	2.06	2.01	23.53	24.06
0.501	1.84	6.58	5.00	2.20	2.37	38.88	38.29
0.329	1.20	5.42	5.47	2.19	2.13	30.75	25.70

Table A-6. Atomization at 1868°F, Triple Injector.

QL/QG	WL/WG	GM	FX	GSD	S	MX	MMD
0.345×10^{-3}	1.26	9.11	9.25	2.07	1.86	29.83	27.08
0.373	1.36	5.44	5.36	1.82	2.01	23.58	22.10
0.411	1.50	6.12	6.25	1.96	2.06	30.21	30.58
0.512	1.87	7.30	7.42	2.10	2.05	35.16	41.22
0.585	2.14	7.29	7.20	2.14	2.22	49.32	46.24
0.669	2.46	5.65	4.93	1.95	2.43	52.74	45.90
0.677	2.48	10.19	10.45	1.83	1.89	35.69	35.00
0.422	1.68	8.88	9.49	1.75	1.81	27.75	31.61
0.294	1.08	6.85	6.97	2.05	1.94	26.08	25.07
0.269	0.981	6.02	6.27	1.89	1.94	23.59	22.08
0.480	1.76	8.08	8.16	2.06	1.99	34.14	45.98
0.374	1.37	5.79	6.09	1.88	1.92	22.22	23.44
0.245	0.893	5.34	5.60	2.26	2.07	27.44	27.49
0.326	1.19	6.90	7.41	1.97	1.88	25.00	24.00
0.424	1.55	7.46	7.51	2.01	1.94	28.28	26.66
0.430	1.57	5.51	5.00	1.87	2.23	35.03	33.92
0.505	1.85	4.74	4.12	1.69	2.14	23.52	21.27
0.113	0.421	4.50	3.59	1.60	2.15	21.27	18.40
0.082	0.300	3.18	2.54	1.91	2.47	29.89	23.02
0.150	0.551	5.05	4.26	1.76	2.25	30.76	31.72

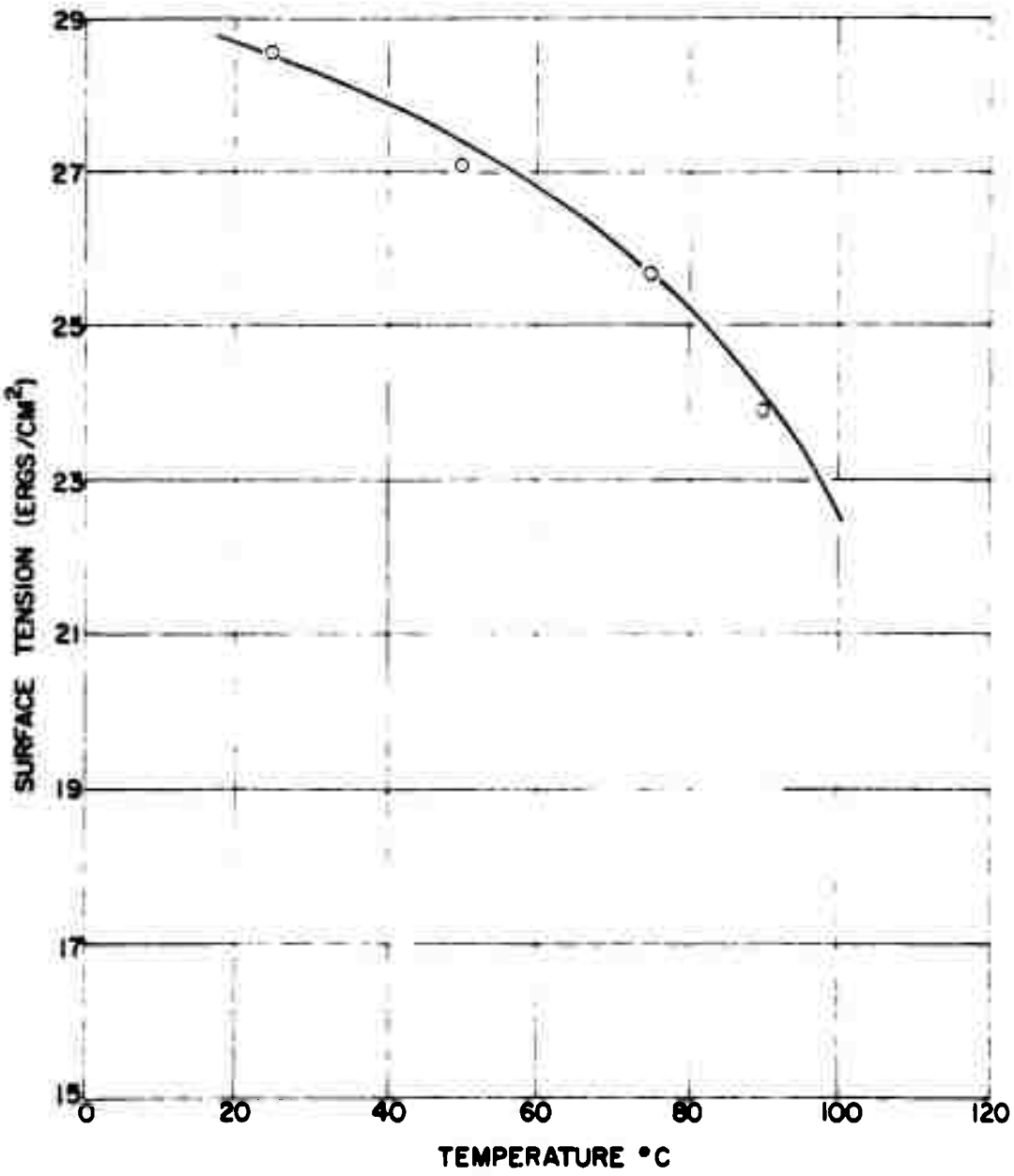

Figure A-1. Surface Tension of Uvinul-Bis Solution.

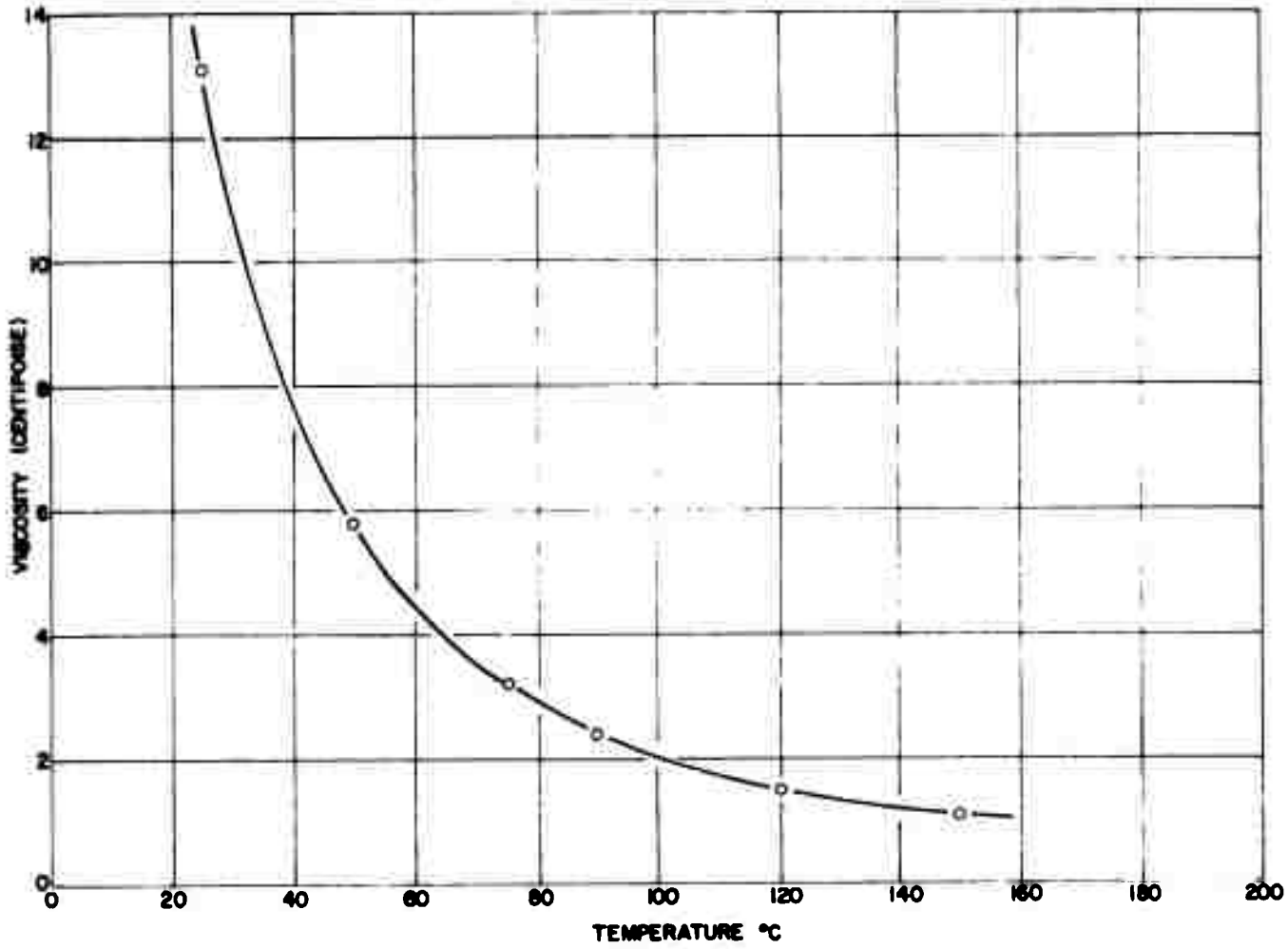

Figure A-2. Viscosity of Uvinul-Bis Solution.

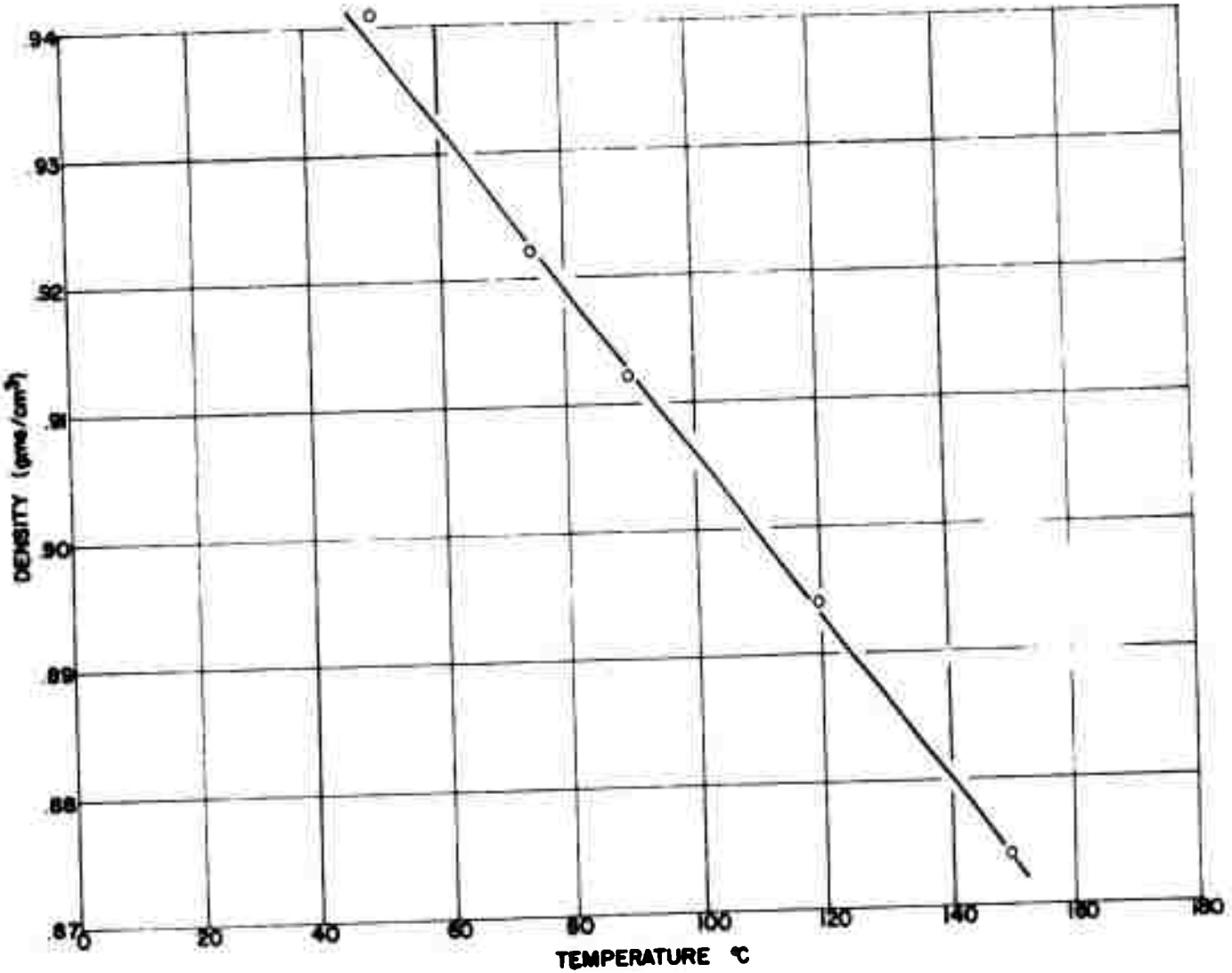

Figure A-3. Density of Uvinul-Bis Solution.